ELSEVIER

Marine Geology 212 (2004) 153–181

MARINE GEOLOGY
INTERNATIONAL JOURNAL OF MARINE GEOLOGY, GEOCHEMISTRY AND GEOPHYSICS

www.elsevier.com/locate/margeo

Methane-related authigenic carbonates from the Black Sea: geochemical characterisation and relation to seeping fluids

A. Mazzini[a,*], M.K. Ivanov[b], J. Parnell[a], A. Stadnitskaia[b,c], B.T. Cronin[a], E. Poludetkina[b], L. Mazurenko[d], T.C.E. van Weering[c]

[a]*Department of Geology and Petroleum Geology, University of Aberdeen, Meston Building, King's College, Aberdeen AB24 3UE, Scotland, UK*
[b]*UNESCO MSU Center for Marine Geology and Geophysics, Faculty of Geology, Moscow State University, Vorobjevy Gory, 119899 Moscow, Russia*
[c]*Royal Netherlands Institute for Sea Research, PO Box 59, 1790 AB Den Burg, The Netherlands*
[d]*All Russia Research Institute for Geology and Mineral Resources of the Ocean, Angliuskiy Avenue, 190121 St. Petersburg, Russia*

Received 22 July 2003; received in revised form 13 July 2004; accepted 26 August 2004

Abstract

During TTR11 Cruise (2001), three areas of active fluid venting and mud volcanism were investigated in the Black Sea below the oxic zone at depths varying between 800 and 2200 m. Authigenic carbonates often associated with microbial mats were recovered from the sea floor and the shallow subsurface. Structural and petrographic observations allowed the distinction of five different types of authigenic carbonates; three of these consist of carbonate-cemented layered hemipelagic sedimentary units, while the other two consist of carbonate-cemented mud breccia sediment and authigenic micrite slabs. The carbonate cements consist predominantly of micritic Mg calcite. Their $\delta^{13}C_{CaCO_3}$ varies between −8.5‰ and −46.9‰ at the different sampling locations, indicating that authigenic carbonates incorporate variable proportions of carbon derived from the anaerobic oxidation of methane (AOM), the oxidation of organic matter and from sea water. Methane is the dominant component among other hydrocarbon gases in these sediments. Its relative amount varies from 99.9% to 95.1% of total hydrocarbon gases and its $\delta^{13}C$ values range from ≅ −40‰ to ≅ −74‰. Methane in sediments associated with the carbonate crusts shows carbon isotopic values 25–30‰ lighter than the authigenic carbonates at all the studied sites, indicating that methane present in the seeping fluids confers a distinct isotopic signature to the carbonate deposits at each location. Models proposed for the formation of carbonate slabs in the subsurface imply methane seepage impeded by homogenous clayey laminae or by pre-existing slabs, coupled with microbial activity oxidising methane and organic matter present in the sediment. Mud breccia crust pavements on the sea floor form by carbonate cementation of methane-charged sediment. Gas saturation of the sediment is confirmed by the presence of gas hydrates, whose shape indicates an association with authigenic carbonates, supporting the idea that sedimentary structures can control gas distribution.

Keywords: Black Sea; authigenic carbonate; hydrocarbon seepage; methane and gas hydrates; mud volcanism

* Corresponding author. Tel.: +44 1224 273435; fax: +44 1224 272785.
E-mail address: a.mazzini@abdn.ac.uk (A. Mazzini).

0025-3227/$ - see front matter © 2004 Elsevier B.V. All rights reserved.
doi:10.1016/j.margeo.2004.08.001

1. Introduction

The Black Sea is a region where well-developed seepage-related structures are widely distributed in deep-water environments. These features are commonly associated with geological structures such as mud diapirs and volcanoes, and fault network systems. Fluid seepage, gas-saturated sediments and authigenic carbonate formation have been observed in various areas on the north-western (Shnukov et al., 1995; Peckmann et al., 2001; Thiel et al., 2001; Michaelis et al., 2002), central and north-eastern (Ivanov et al., 1989, 1992, 1998; Ginsburg et al., 1990; Konyukhov et al., 1990; Limonov et al., 1994; Woodside et al., 1997; Kenyon et al., 2002; Blinova et al., 2003; Bohrmann et al., 2003), and south-eastern (e.g., Kruglyakova et al., 1993; Cifci et al., 2002; Ergun et al., 2002) parts of the Black Sea. Methane release can occur in large quantities (high-intensity vents) generating dense bubble curtains or plumes (Michaelis et al., 2002), or it can be "normal" (cold seeps) with a large part of the methane dissolved and oxidised (Amouroux et al., 2002; Ivanov et al., 2002; Lein et al., 2002), consumed by microorganisms, and fixed on the sea floor as carbonate crusts.

Authigenic carbonate deposits have been documented in several areas where active mud volcanism take place (e.g., Le Pichon et al., 1990; Vogt et al., 1997; Ivanov, 1999; Aloisi et al., 2000), and where the large amount of methane rising provides an ideal location for the formation of gas hydrates when P/T conditions are advantageous (e.g., Carson et al., 1990, 1994; Ivanov et al., 1996; Bohrmann et al., 1998, 1998; Ginsburg et al., 1999). The precipitation of authigenic carbonates is inferred to be the result of coupled anaerobic methane oxidation (AOM) and sulphate reduction (e.g., Ritger et al., 1987) operated by a consortium of archaea and sulphate-reducing bacteria (e.g., Boetius et al., 2000; Michaelis et al., 2002).

During the 11th Training Through Research cruise, mud volcanoes and cold seeps of the Black Sea were investigated with the Russian R/V *Professor Logachev*. This paper focuses on petrography and geochemistry of a large collection of authigenic carbonates slabs and sediments and proposes mechanisms of formation for authigenic carbonates formed at the explored locations.

2. Geological setting and study areas

The Black Sea is the world's largest anoxic marine basin. Structurally, it consists of two basins (Eastern and Western Black Sea basins) separated by the Andrusov Ridge. Five main seismic sedimentary units within the Black Sea are known: Upper Cretaceous (carbonates), Palaeocene–Eocene (siliciclastic and carbonate rocks), Oligocene–Lower Miocene (Maikopian Formation clays), Upper Miocene (siliciclastic), and Pliocene–Quaternary consisting of mostly clays (Tugolesov et al., 1985; Nikishin et al., 2003).

Recent events in the basin caused its anoxic nature. In fact, the Holocene global sea level rise allowed the invasion of high salinity waters from the Mediterranean into the Black Sea via the Bosphorus, approximately 9000 years BP (Ross et al., 1970) or about 7000 years BP (Ryan et al., 1997). Permanent stratification was established between the original fresh water body and the underlying marine waters, allowing anoxia to develop in the bottom layers accompanied by a slow rise of the halocline (Ross and Degens, 1974). At present, 80% of the water column is anoxic. The oxic–anoxic interface zone varies in depth between 130 and 180 m (Ross et al., 1978).

During the 11 years of activity of the TTR program, several cruises have been made in the Black Sea. The central part was investigated during TTR1 (Ivanov et al., 1992), TTR3 (Limonov et al., 1994), and TTR6 (Woodside et al., 1997). The Sorokin Trough and Caucasus continental margin were studied during TTR6 (Woodside et al., 1997). The aim of the TTR-11 cruise (Kenyon et al., 2002) was to further investigate three areas previously explored in the framework of the TTR program (Fig. 1) characterised by the presence of gas hydrates, hydrocarbon fluid seeps, and mud volcanism, paying particular attention to geochemical and microbiological processes.

Area 1 is located in the northwestern part of the continental slope of the Black Sea situated offshore SW Crimean peninsula and south of Ukraine. The region comprises several manifestations of gas venting (e.g., Polikarpov et al., 1993; Bohrmann et al., 2002; Ivanov et al., 2002; Gulin et al., 2003). The sampling was concentrated in two main regions: the

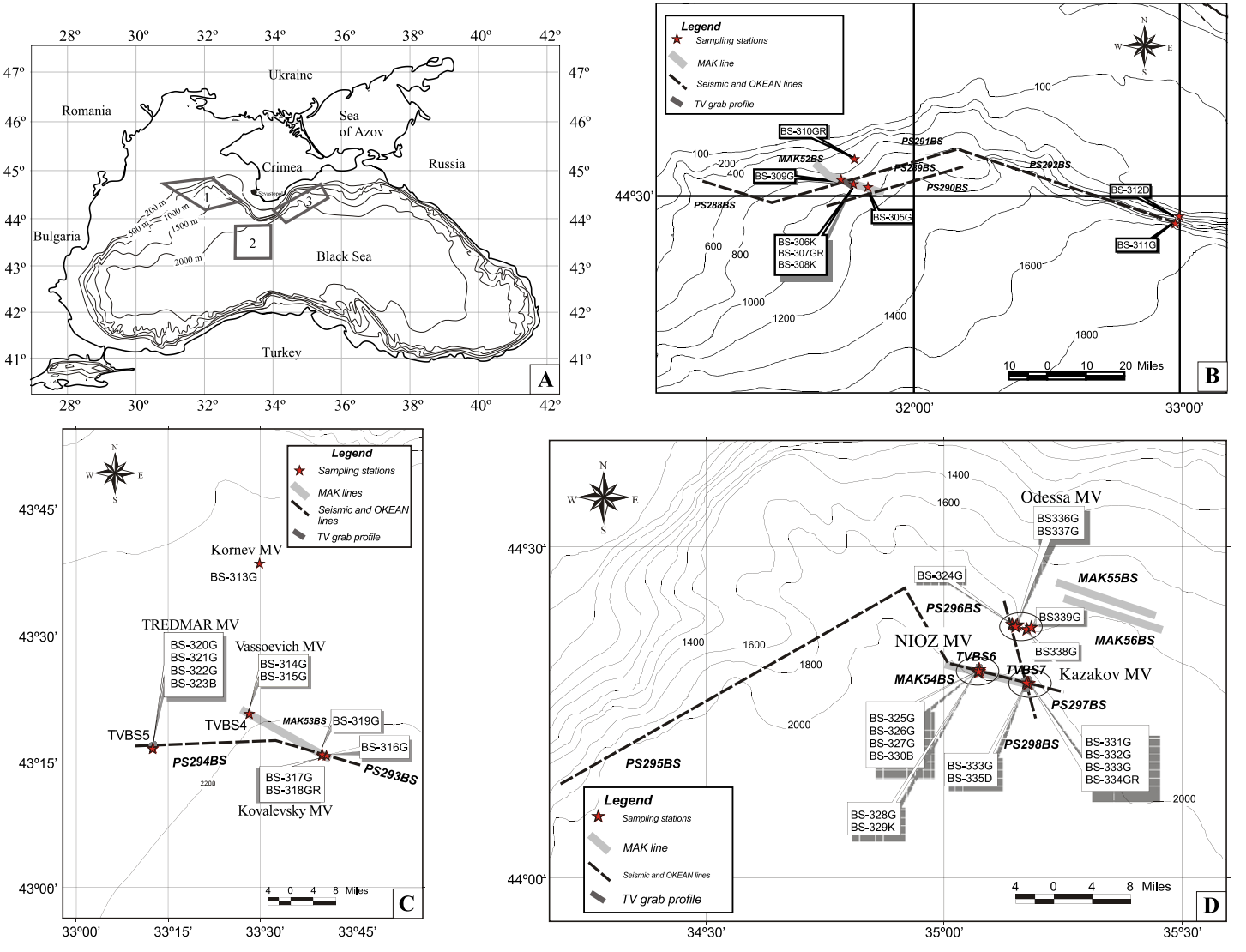

Fig. 1. (A) Black Sea and main study areas investigated during the TTR-11 cruise. (B) Area 1 (Kalamitian continental slope and Crimean continental slope). (C) Area 2 (central Black Sea). (D) Area 3 (Sorokin Trough).

Kalamitian continental slope and a section westward of Sevastopol. Acoustic images of the area show fields of patches with high backscatter on the sidescan sonar profile that showed a superficial transparent layer underneath a very strong reflector on the subbottom profiler. Similar features were observed nearby on seismic profiles (Kenyon et al., 2002). Here, faults and vertical transparent areas and masked reflectors suggest the presence of gas. Faults seen on the subbottom profiler records underneath these fields are believed to be the conduits for fluids migrating upwards (Kenyon et al., 2002).

Area 2 is situated in the central part of the Black Sea on the western side of the Andrusov Ridge (Fig. 1). This region, located in the deepest part of the western Black Sea basin, shows generally flat seafloor topography with water depths of 2100–2200 m. The north-eastern part of the region includes a large mud volcano field, comprising nine structures, broadly studied during previous TTR cruises. Three of them, including the TREDMAR, Vassoevich and Kovalevsky mud volcanoes, were studied during the survey presented here. Seismic records suggest deep sources for the mud volcanism, and various acoustic anomalies observed indicate multilevel gas accumulations within the mud breccia (Kenyon et al., 2002).

Area 3 is situated on the southeastern continental slope of the Crimean Peninsula, where the Sorokin Trough becomes elongate (Fig. 1). This area of compressional regime (Limonov et al., 1997) represents a special geochemical setting due to multiple manifestations of gas venting, the occurrence of mud volcanoes, sub-bottom methane hydrates, and possibly free gas preservation in near-bottom sediments (Limonov et al., 1997; Woodside et al., 1997; Bouriak and Akhmetjanov, 1998; Ivanov et al., 1998). Mud volcano deposits, from which authigenic carbonates were recovered, are composed of mud breccia of different lithological types, overlain in some cases by thin, stratified recent sediments. Elevated concentrations of hydrocarbon gas and hydrogen sulphide occur in almost all carbonate deposition sites (Ivanov et al., 1998). During the TTR-11 cruise, Kazakov mud volcano was intensively sampled and three other previously explored structures were proven to have a mud volcanic origin (Kenyon et al., 2002). These structures were named Tbilisi, NIOZ, and Odessa.

3. Recent sedimentation in the Black Sea

In 1969, Cruise 49 of Atlantis II (Degens and Ross, 1972) confirmed that a common pattern, including three distinct modern sedimentary units, characterised most of the deep-water areas of the Black Sea. Below the surface, the typical geological sequence includes three units. The shallowest Unit 1 (Djemetinian layers) consists of thin alternating coccolithic ooze (mostly Emiliana huxleyi), and clayey sediment laminae; Unit 2 (Kalamitian layers) consists almost entirely of thin laminations of sapropel with occasional coccolithic ooze laminae; Unit 3 (Novoeuxinian layers), interpreted to be a lacustrine facies, consists of laminations of terrigenous clayey material, sometimes with abundant silty admixture, sometimes very fine and well sorted, commonly containing hydrotroilite layers. These units reach their maximum thickness in the central part of the Black Sea; Units 1 and 2 are on average 30-cm thick, while Unit 3 can reach several metres in thickness (Ross and Degens, 1974). These units were retrieved in all three study areas. The majority of the authigenic carbonates described in the paper were retrieved from these units.

4. Methods

Petrographic and geochemical analyses were conducted on the authigenic carbonate samples complemented by geochemical studies of gases and pore waters of the enclosing sediments. A large suite of polished thin sections was prepared cutting each sample perpendicular and parallel to the sedimentary layer. Polished slabs and thin sections were studied using standard petrographic and cathodoluminescence techniques and freshly broken rock samples were examined with scanning electron microscope (SEM). Samples for carbon and oxygen stable isotope measurements were drilled systematically along the thickness of the samples from the different textures and layers observed within the slabs. Oxygen and carbon stable isotopes measurements were performed liberating CO_2 by the standard phosphoric acid technique (MaCrea, 1950; Sharma and Clayton, 1965). Measurements were made with a Carbonate Prep System linked with an AP2003 mass spectrometer. The $\delta^{13}C$ and $\delta^{18}O$ results are reported relative

to the V-PDB standard (Craig, 1957; Coplen, 1994), the precision of the analyses is ±0.2‰. The Friedman and O'Neil (1977) fractionation equation was used to calculate the temperatures of carbonate precipitation. Semiquantitative mineralogical composition of the carbonate phase in carbonate precipitates was determined by X-ray diffraction (XRD) (Shlikov and Kharitonov, 2001). Gas and pore water were extracted from the sediments at selected depths (every 10 cm or where significant lithological variations were observed) and analysed. Volumes of 40 ml of sediment were degassed using the head space technique (Bolshakov and Egorov, 1987) and the relative hydrocarbon gas compositional analyses (from C1 to C5) were carried out using a Tzvet-500 chromatograph with ionising detector (Jeffery and Kipping, 1976). The values of methane concentrations are given in ml/l of wet sediment. The stable carbon isotopic composition of methane was measured on a Finnigan Delta S mass spectrometer with a HP 5890 GC and a GC-Combustion interface. Methane was separated on a molsieve 5A plot column using split- or splitless injection, depending on the concentrations. Chemical analyses of the pore water samples extracted onboard were carried out according to Reznikov and Muikovskaya (1956), McDuff (1985), and Gieskes et al. (1991). Chloride (Cl), alkalinity, Ca, and Mg were determined titrimetrically (argento-, acide-, and complexometry, respectively). The accuracy of the chemical analyses was estimated at ±0.01 mg/l.

5. Results

A total of 35 stations were sampled in the anoxic zone of the three study areas where acoustic data interpretation inferred the presence of gas-charged sediments or fluid seepage/sediment extrusions (i.e., mud volcanoes). Several active fluid seepage features and numerous mud volcanoes, including the Kornev, Vassoevich, Kovalevsky, TREDMAR (Area 2), Tbilisi, NIOZ, Kazakov, and Odessa (Area 3), were sampled. Most of the features revealed a strong smell of H_2S. A large collection of carbonate-cemented sedimentary units and other authigenic carbonate-cemented slabs was retrieved from these locations. Detailed petrographic and geochemical studies of the authigenic carbonates allowed a new classification of the different samples retrieved.

5.1. The hydrocarbon gas composition

The majority of the gas analyses (Table 1; Figs. 2 and 10, top) were determined for samples from the same seepage features where carbonate crusts were retrieved.

It is worthy of note that in spite of the absolute notations for the methane, part of the hydrocarbon had been lost due to active degassing of the recovered sediments. However, in order to see the trend of methane distribution profiles and to show a rough level of methane saturation even with its loss, it was decided to present methane data in both absolute (ml/l of wet sediment) and relative (% from total determined hydrocarbon gases) values.

In Area 1, the gas composition was determined from sediments extracted from a long core (BS-311G) retrieved on the Crimean continental slope west of Sevastopol, which consisted entirely of hemipelagic sediments. The hydrocarbon gas composition is represented by a set of alkanes from methane to butane (C_1–C_4) where alkanes are predominant over alkenes (ethene and propene) and *i*-butane prevailing under *n*-butane. Propane (C_3) and butane (C_4) have significant concentrations only in the lower part of the sedimentary sequence (below 500 cm). Concentrations of methane varied from 1 ml/l in the upper part of the core to 90 ml/l in the lower part (Fig. 2A). The isotopic composition of methane was measured from a short (150 cm) core (BS-308 K). Results did not show a strong variation between the three different sedimentary units analysed. Values showed a strong ^{13}C depletion in the upper part of the core ($\delta^{13}C_{CH4}$= −74.2‰) and less depleted values for the rest of the core (as low as −67.3‰).

The three mud volcanic structures (Vassoevich, Kovalevsky, and TREDMAR) sampled in Area 2 showed very similar gas compositions and concentrations to each other. For the Vassoevich mud volcano, the hydrocarbon gas mixture was represented by a set of alkanes from methane (C_1) to butane (C_4) (Fig. 2B), and for the Kovalevsky and TREDMAR mud volcanoes methane (C_1) to pentane (C_5) (Fig. 2C–D) all containing saturated, unsaturated alkanes

Table 1
Summary of analyses carried out on this study from a large collection of authigenic carbonates and cores

Area	Sampling station no.	Structure	Depth BSF (cm)	$\delta^{18}O$	$\delta^{13}C$ (authigenic carbonate)	$\delta^{13}C$ (CH_4)	Authigenic carbonate type or sediment type	XRD, carbonate cement composition (%)	Sampling points for isotope analyses
1	BS-306-K	Faulted seepage feature	4	2.3	−44.1		Type U1a		Small tabular fragment, top surface
1	BS-306-K	Faulted seepage feature	4	1.1	−43.8		Type U1a		Small tabular fragment, top surface
1	BS-306-K	Faulted seepage feature	4	0.6	−43.2		Type U1a	14.7 LMC, 85.3 HMC	Small tabular fragment, top surface
1	BS-306-K	Faulted seepage feature	25	−2.6	−25.6		Type MSb		Small tabular fragment, top surface
1	BS-306-K	Faulted seepage feature	25	−2.5	−26.8		Type MSb		Small tabular fragment, bottom surface
1	BS-308-K	Faulted seepage feature	10	1.4	−43.5		Type U1b		Top surface of the slab
1	BS-308-K	Faulted seepage feature	10	0.9	−46.9		Type U1b		Bottom surface of the slab
1	BS-308-K	Faulted seepage feature	10	1.3	−46.2		Type U1b		Bottom surface of the slab
1	BS-308-K	Faulted seepage feature	10			−74.2	Clay, Unit 1		Middle part of Unit 1
1	BS-308-K	Faulted seepage feature	15			−68.8	Sapropel, Unit 2		Middle part of Unit 2
1	BS-308-K	Faulted seepage feature	20			−65.7	Clay, Unit 3		Middle part of Unit 3
2	BS-314-G	Vassoevich M.V.	4	1.0	−8.5		Type U1b		Central part of the slab
2	BS-314-G	Vassoevich M.V.	4	0.9	−9.2		Type U1b		Central part of the slab
2	BS-314-G	Vassoevich M.V.	4	1.4	−10.5		Type U1b	37.7 LMC, 62.3 HMC	Central part of the slab
2	BS-314-G	Vassoevich M.V.	26	0.7	−16.4		Type U2a	100 HMC	Central part of the slab
2	BS-314-G	Vassoevich M.V.	26	1.3	−17.0		Type U2a		Central part of the slab
2	BS-314-G	Vassoevich M.V.	26	1.0	−18.0		Type U2a		Central part of the slab
2	BS-314-G	Vassoevich M.V.	33	0.5	−18.3		Type U3		Central part of the slab
2	BS-314-G	Vassoevich M.V.	65–70			−56.2	Clay, Unit 3		Top part of Unit 3
2	BS-315-G	Vassoevich M.V.	24	1.6	−24.2		Type U2b		Central part of the slab
2	BS-315-G	Vassoevich M.V.	24	1.0	−24.5		Type U2b		Top surface of the slab
2	BS-315-G	Vassoevich M.V.	24	1.5	−20.1		Type U2b		Central part of the slab
2	BS-315-G	Vassoevich M.V.	24	1.1	−22.6		Type U2b	100 HMC	Central part of the slab
2	BS-315-G	Vassoevich M.V.	65	1.6	−23.5		Type U2b		Central part of the slab
2	BS-315-G	Vassoevich M.V.	65	1.5	−22.1		Type U2b		Bottom surface of the slab
2	BS-315-G	Vassoevich M.V.	65	1.7	−22.6		Type U2b		Top surface of the slab
2	BS-315-G	Vassoevich M.V.	65	1.4	−21.6		Type U2b	100 HMC	Central part of the slab
2	BS-317-G	Kovalevsky M.V.	28	−0.2	−17.2		Type U1a	44.3 LMC, 55.7 HMC	Central part of the slab
2	BS-319-G	Kovalevsky M.V.	120–125			−31.6	Mud breccia sediment		Mud breccia unit
2	BS-319-G	Kovalevsky M.V.	196–223			−49.8	Mud breccia sediment		Mud breccia unit
2	BS-319-G	Kovalevsky M.V.	250			−39.8	Mud breccia sediment		Mud breccia unit
2	BS-320-G	TREDMAR M.V.	145–153			−50.7	Mud breccia sediment		Mud breccia unit

Table 1 (*continued*)

Area	Sampling station no.	Structure	Depth BSF (cm)	$\delta^{18}O$	$\delta^{13}C$ (authigenic carbonate)	$\delta^{13}C$ (CH_4)	Authigenic carbonate type or sediment type	XRD, carbonate cement composition (%)	Sampling points for isotope analyses
3	BS-324-G	Diapiric structure	4	1.0	−39.1		Type U1b		Central part of the slab
3	BS-324-G	Diapiric structure	4	0.7	−37.6		Type U1b		Top surface of the slab
3	BS-324-G	Diapiric structure	4	1.0	−38.7		Type U1b		Bottom surface of the slab
3	BS-324-G	Diapiric structure	4	0.2	−38.4		Type U1b	100 HMC	Central part of the slab
3	BS-325-G	NIOZ M.V.	0–4			−66.0	Mud breccia sediment		Mud breccia unit
3	BS-325-G	NIOZ M.V.	8–11			−67.4	Mud breccia sediment		Mud breccia unit
3	BS-325-G	NIOZ M.V.	22–27			−60.7	Mud breccia sediment		Mud breccia unit
3	BS-325-G	NIOZ M.V.	52–57			−59.9	Mud breccia sediment		Mud breccia unit
3	BS-325-G	NIOZ M.V.	88			−59.9	Mud breccia sediment		Mud breccia unit
3	BS-326-G	NIOZ M.V.	19	0.4	−41.2		Type U1b		Central part of the slab
3	BS-326-G	NIOZ M.V.	37	−0.6	−33.5		Type MSb	34.8 LMC, 65.2 HMC	Top surface of tabular slab
3	BS-326-G	NIOZ M.V.	190			−67.1	Hemipelagic slumped clay		Bottom part of core
3	BS-327-G	NIOZ M.V.	5	1.2	−40.5		Type MSb	16.3 LMC, 83.7 HMC	Top surface of tabular slab
3	BS-327-G	NIOZ M.V.	90			−49.1	Hemipelagic slumped clay		Gas hydrates bearing layer
3	BS-331-G	Kazakov M.V.	20–25			−55.3	Mud breccia sediment		Mud breccia unit
3	BS-331-G	Kazakov M.V.	40–45			−55.3	Mud breccia sediment		Mud breccia unit
3	BS-331-G	Kazakov M.V.	81–86			−55.6	Mud breccia sediment		Mud breccia unit
3	BS-331-G	Kazakov M.V.	101–103			−55.9	Mud breccia sediment		Mud breccia unit
3	BS-331-G	Kazakov M.V.	138–142			−56.1	Mud breccia sediment		Mud breccia unit
3	BS-331-G	Kazakov M.V.	165			−56.0	Mud breccia sediment		Mud breccia unit
3	BS-333-G	Kazakov M.V.		0.7	−17.6		Type U1a	100 HMC	Small tabular fragment, top surface
3	BS-334-GR	Kazakov M.V.		1.3	−18.8		Type U1a		Top surface of the slab
3	BS-334-GR	Kazakov M.V.		1.7	−19.3		Type U1a		Central part of the slab
3	BS-334-GR	Kazakov M.V.		1.3	−19.3		Type U1a		Top surface of the slab
3	BS-334-GR	Kazakov M.V.		1.5	−19.8		Type U1a		Bottom surface of the slab
3	BS-334-GR	Kazakov M.V.		1.5	−20.1		Type U1a		Bottom surface of the slab
3	BS-334-GR	Kazakov M.V.		1.6	−22.1		Type U1b		Central part of the slab

(continued on next page)

Table 1 (*continued*)

Area	Sampling station no.	Structure	Depth BSF (cm)	$\delta^{18}O$	$\delta^{13}C$ (authigenic carbonate)	$\delta^{13}C$ (CH_4)	Authigenic carbonate type or sediment type	XRD, carbonate cement composition (%)	Sampling points for isotope analyses
3	BS-334-GR	Kazakov M.V.		1.4	−22.5		Type U1b		Bottom surface of the slab
3	BS-334-GR	Kazakov M.V.		1.3	−19.3		Type MSa		Central part of the slab
3	BS-334-GR	Kazakov M.V.		0.7	−20.1		Type MSa		External soft surface of the slab
3	BS-334-GR	Kazakov M.V.		1.4	−19.2		Type MSa		External hard surface of the slab
3	BS-334-GR	Kazakov M.V.		1.1	−20.8		Type MSa		Top surface of the slab
3	BS-334-GR	Kazakov M.V.		1.4	−22.0		Type MB		External surface of crust
3	BS-334-GR	Kazakov M.V.		2.1	−20.5		Type MB		External surface of crust
3	BS-334-GR	Kazakov M.V.		1.2	−16.7		Type MB		External surface of crust
3	BS-334-GR	Kazakov M.V.		1.6	−22.1		Type MB	9.5 LMG, 90.5 HMC	External surface of crust
3	BS-335-D	Kazakov M.V.		1.6	−16.6		Type U1a		Central part of the slab
3	BS-335-D	Kazakov M.V.		1.5	−15.6		Type U1a		Top surface of the slab
3	BS-335-D	Kazakov M.V.		1.4	−18.1		Type U1a		Bottom surface of the slab
3	BS-335-D	Kazakov M.V.		−1.7	−15.3		Type MB		Central part of the slab
3	BS-335-D	Kazakov M.V.		0.5	−23.1		Type MB		Top surface of the slab
3	BS-335-D	Kazakov M.V.		1.1	−22.5		Type MB	100 HMC	External surface
3	BS-335-D	Kazakov M.V.		0.6	−20.1		Type MSa	22.3 LMC, 77,7 HMC	Central part of the slab
3	BS-335-D	Kazakov M.V.		1.1	−20.5		Type MSa		Central part of the slab
3	BS-335-D	Kazakov M.V.		0.3	−19.2		Type MSa		Top surface of the slab
3	BS-335-D	Kazakov M.V.		0.9	−20.3		Type MSa		Bottom surface of the slab
3	BS-336-G	Odessa M.V.	12	1.1	−44.7		Type U2b	100 HMC	Central part of the slab
3	BS-336-G	Odessa M.V.	62	−1.8	−15.5		Type MSb	80 LMC, 20 DOL	Central part of the slab
3	BS-336-G	Odessa M.V.	0–17			−69.9	Clay, Unit 1		Middle part of Unit 1
3	BS-336-G	Odessa M.V.	20–27			−67.5	Clay, Unit 3		Upper part of Unit 3
3	BS-336-G	Odessa M.V.	30–37			−67.9	Clay, Unit 3		Middle part of Unit 3
3	BS-336-G	Odessa M.V.	50–55			−67.1	Clay, Unit 3		Middle part of Unit 4
3	BS-336-G	Odessa M.V.	67–72			−70.4	Clay, Unit 3		Hydrotrilite rich interval
3	BS-336-G	Odessa M.V.	130–135			−66.5	Clay, Unit 3		Hydrotrilite rich interval
3	BS-336-G	Odessa M.V.	140–145			−66.6	Clay, Unit 3 ?		Hydrotrilite rich interval
3	BS-337-G	Odessa M.V.	35	−0.1	−44.9		Type U2b		Central part of the slab
3	BS-337-G	Odessa M.V.	35	1.4	−45.5		Type U2b		Bottom surface of the slab
3	BS-337-G	Odessa M.V.	35	1.0	−44.1		Type U2b		Top surface of the slab
3	BS-337-G	Odessa M.V.	80	−0.3	−40.8		Type MSb		Central part of the slab
3	BS-337-G	Odessa M.V.	80	−0.6	−35.5		Type MSb		External surface of the slab
3	BS-337-G	Odessa M.V.	80	−0.2	−40.4		Type MSb		Central part of the slab
3	BS-337-G	Odessa M.V.	80	−0.6	−38.7		Type MSb		Central part of the slab
3	BS-337-G	Odessa M.V.	80	−0.4	−41.3		Type MSb		Central part of the slab
3	BS-337-G	Odessa M.V.	80	0.2	−37.6		Type MSb	29.3 LMC, 70.7 HMC	Central part of the slab

HMC=high Mg calcite; LMC=low Mg calcite; DOL=dolomite; K=Kasten corer; G=gravity corer; D=dredge; Gr=TV remote controlled grab.

and *i*-butane. The ratio of methane to its homologues (C_{2+}) varied from 1500 to 12000. Gas measurements from the mud breccia units revealed high concentrations of methane, up to 130, 90, and 70 ml/l, respectively, with low values only from the capping hemipelagic unit. Methane from the Vassoevich and the TREDMAR mud volcanoes had low $\delta^{13}C_{CH4}$ values (−56.2‰ and −50.7‰, respectively), compared to the methane from the Kovalevsky mud volcano (from −31.6‰ to −49.8‰).

In Area 3, the NIOZ, Kazakov, and Odessa mud volcanoes were studied. Mud breccia cores from the NIOZ mud volcano revealed the presence of hydrocarbon gases from methane (C_1) to propane (C_3), unsaturated homologues in small concentrations and methane concentrations up to 56 ml/l (Fig. 2E). $\delta^{13}C_{CH4}$ varied from −49.1‰ to −67.4‰, although most of the samples have values around −60‰. The hydrocarbon gas mixture of the Kazakov mud volcano was represented by all hydrocarbons from methane (C_1) to pentane (C_5) in each of the studied samples. The content of C_{2+} hydrocarbon gases reached 7%. Ethene and propene were nearly absent. The methane concentration varied from 3 to 56 ml/l (Fig. 2F) and its $\delta^{13}C_{CH4}$ values varied from −55.3‰ to −56.1‰. The hydrocarbon gases from the Odessa mud volcano include hydrocarbons from methane (C_1) to pentane (C_5). Ethene and propene were present in relatively small amounts, and *n*-alkanes were predominant over *iso*-alkanes. In this case, the methane concentration reached 51 ml/l (Fig. 2G). The $\delta^{13}C_{CH_4}$ results gave consistent low values (from −66.5‰ to −70.4‰).

5.2. Morphologies of gas hydrates in the sediments

Gas hydrates were retrieved from all the three areas investigated and were usually associated with authigenic carbonates.

In Area 1, one of the high backscattering patches (500-m wide) observed on the sidescan-sonar profile was sampled. The presence of gas that migrates through the sedimentary column along fault planes was inferred from the acoustic profiles. During the retrieval of the gravity core onto the ship's deck, a large plume of gas bubbles was observed breaking onto the sea surface. Small fragments were observed floating on the surface suggesting that the core contained gas hydrates that partly dissociated during transit from the sea floor to the surface. The same location, sampled with the kasten corer, retrieved slabs of carbonate crust and hemipelagic sedimentary sequence. Hydrates were recovered for the first time in this part of the Black Sea from sediments not associated with a mud volcano (as opposed to what is observed in the rest of the Black Sea) at a water depth of 900 m. The small tabular fragments of gas hydrate (1–2-cm long and 2–3-mm thick) were observed to be distributed as thin laminae oriented along the original lamination of the sapropelic sediments, suggesting that the gas is preferentially trapped along the interface of the sedimentary impermeable units.

In Area 2, the seismic profile of the Kovalevsky mud volcano showed bright spots present at different depths in the feeder channel of the volcano, suggesting the presence of free gas. A "porphyraceus" structure of gas hydrates was observed within the mud breccia unit of the Kovalevsky mud volcano. The aggregates observed consisted of isometric and subrounded pore-filling clathrates whose size varied from millimetric up to 3 cm. Similarly shaped hydrates were observed in the Yuma and Ginsburg mud volcanoes (Moroccan margin) and were interpreted to be the result of the segregation of water by gas supplied into the hydrate accumulation zone (Mazurenko et al., 2003).

Two of the mud volcanic structures (Kazakov and Odessa) sampled in the Sorokin Trough (Area 3) contained gas hydrates. Hydrates retrieved from the Kazakov mud volcano were irregularly leaf-shaped (up to 3 cm in size), usually associated with the thin veneer of laminated hemipelagic sediment occasionally covering the mud breccia unit, or were observed as pore-filling microaggregates in the mud breccia unit like those observed in the mud breccia unit of the Kovalevsky mud volcano, or to the one described by Bohrmann et al. (2002) in the same area (Dvurechenskii mud volcano) or by Stadnitskaia and Belenkaya (1998). Hydrates retrieved from the Odessa mud volcano were found in the hemipelagic sediment (Fig. 3A). Similar to the hydrates retrieved from Area 1, they assumed a tabular shape (from 2 to 3 mm in thickness, up to 5 cm in diameter) and were situated at the interface between the sedimentary layers.

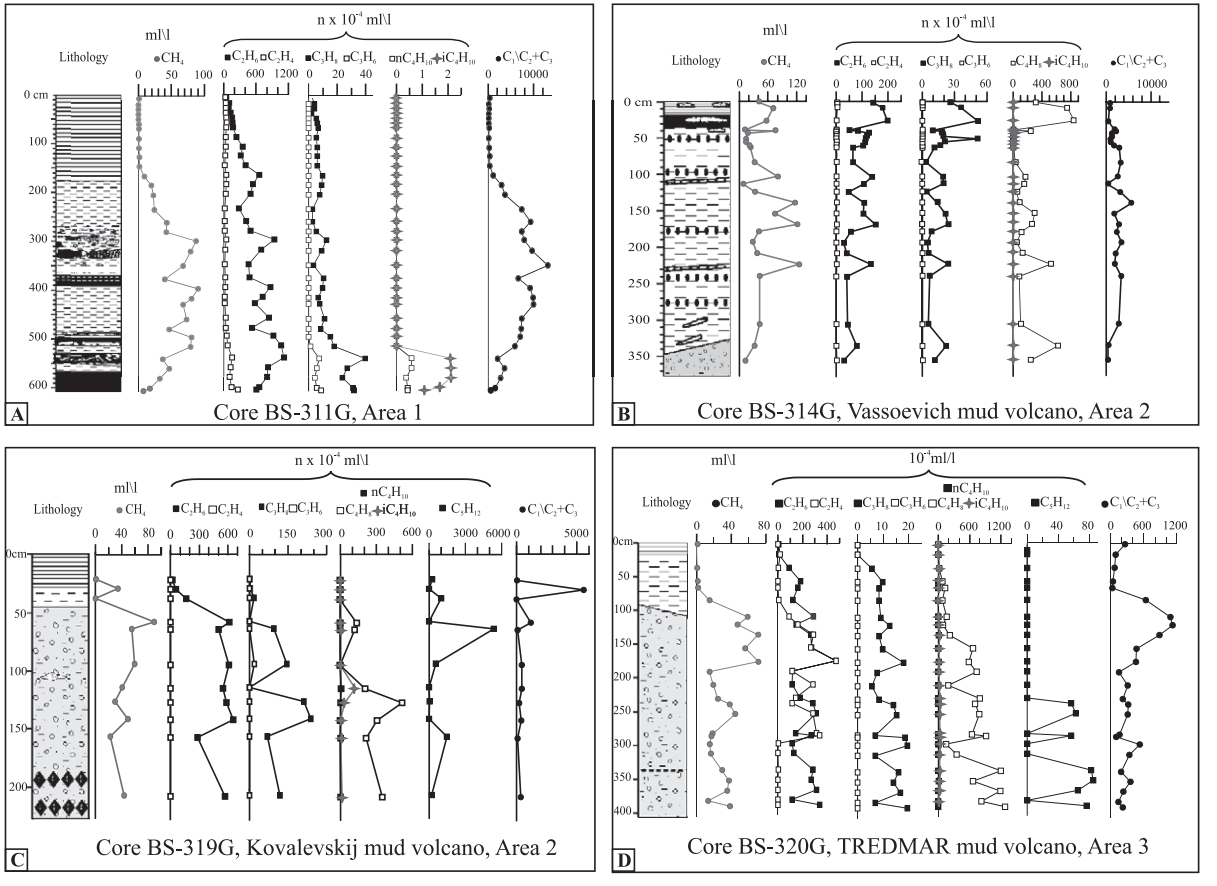

Fig. 2. Summary of results of the hydrocarbon phase gas compositional analyses of the main cores studied and related core logs.

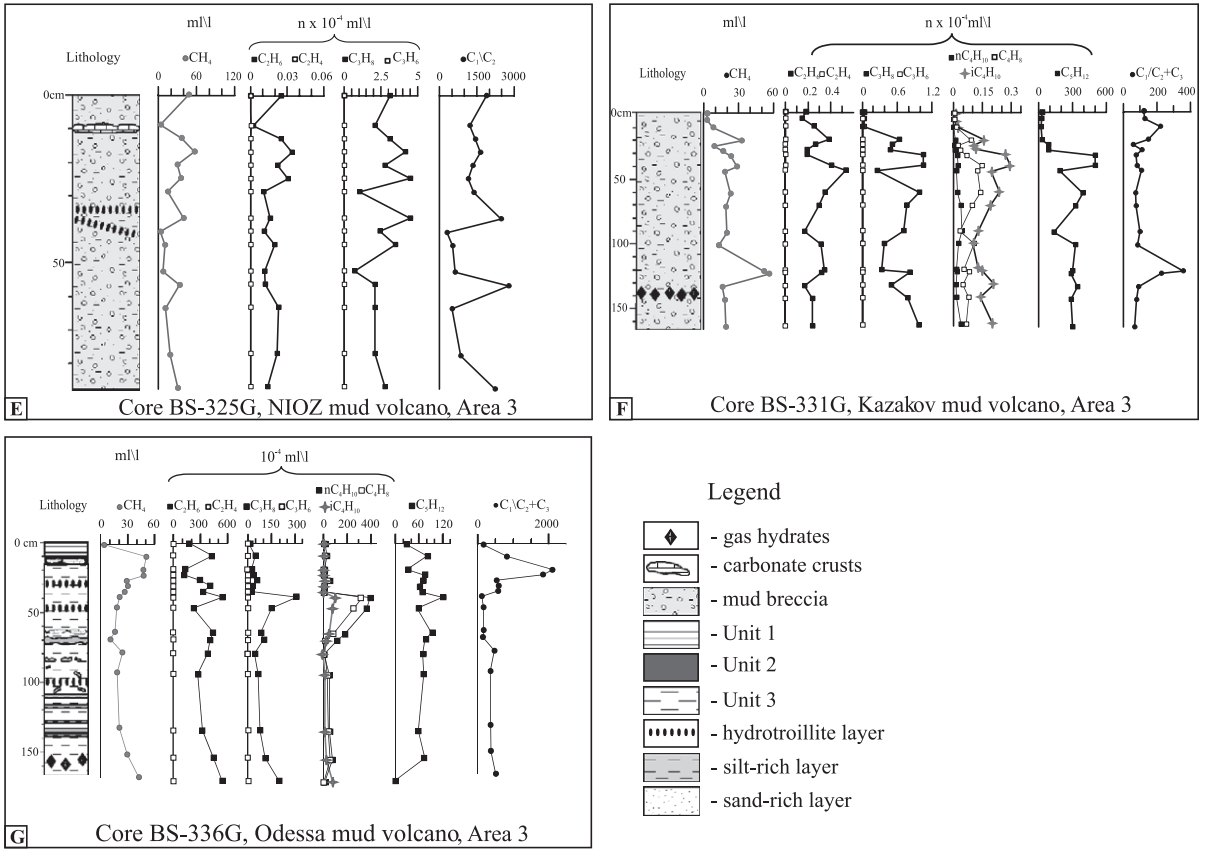

Fig. 2 (*continued*).

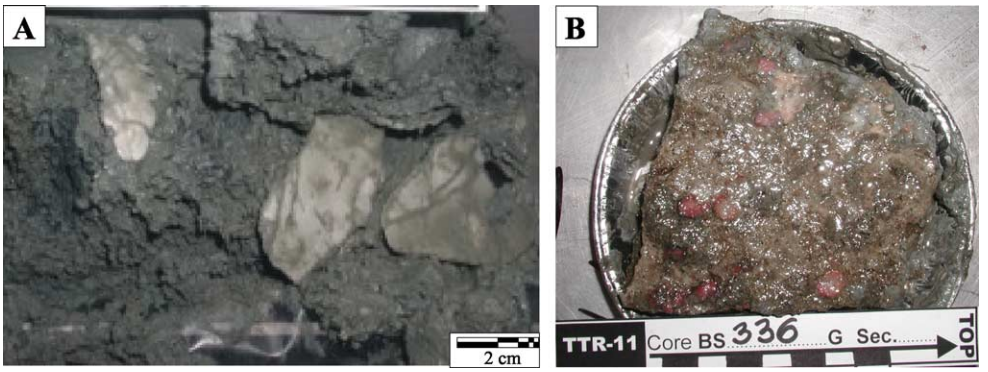

Fig. 3. (A) Tabular-shaped gas hydrates (in lighter colour), oriented along the original lamination of sediments and forming on the interface between the sedimentary layers; (B) microbial mat observed on carbonate-cemented sedimentary slabs; the thickness of the pinkish brown mucous mat increases around the degassing vesicles. (For interpretation of the references to colour in this figure legend, the reader is referred to the web version of this article.)

5.3. Microbial mats associated with authigenic carbonates

Thick microbial mats associated with carbonate slabs were retrieved from several sampling stations. Two different types of mats were observed and they appeared to have similar characteristics to those described by Belenkaya (2003) and Ivanov et al. (1998). The first type showed a pinkish-brown colour and was found growing on the external surfaces of the cemented units and occasionally between the carbonate cemented layers. The most spectacular mats of this type were observed on the lower surface of the well micrite-cemented sapropelic unit (i.e., from the Odessa mud volcano, Fig. 3B). The second type consisted of brownish pore-filling jelly matter observed in several instances filling the degassing features or enclosed in the interface between the sedimentary layers.

5.4. Authigenic carbonates

5.4.1. Petrography of authigenic carbonates

Based on macroscopic and microscopic observations, a new classification of cemented slabs is proposed. Five types of cemented slabs were recognised. The first three types consist of layered samples of cemented sedimentary units (i.e., Unit 1 to 3). The fourth type consists of cemented mud breccia and the fifth comprises structureless micritic slabs. The suffix a or b was added to the type of cemented slab representing poor and good cementation, respectively.

- Type U1—This type of slab consists of cemented Unit 1 and was commonly retrieved from the top and the lower part of the youngest sedimentary Unit 1. The slabs can be subdivided in two subtypes. Subtype U1a is composed of very friable and poorly cemented sedimentary Unit 1 and is light grey in colour (Fig. 4A). The porous slabs preserved the millimetric sedimentary laminae and their subparallel orientation. The laminations that compose the slabs consist of alternations of clay- and carbonate-rich layers. The external uneven flat-like surfaces show microbial remains-filled micro-vesicles whose origin is ascribed to gas seepage. Thin section petrography shows layers of clayey sediment that are separated by mostly continuous biofilm and micrite-rich intervals (Fig. 4B). The better cemented subtype U1b displays a greater amount of micrite filling the pores (Fig. 4C). Pyrite framboid aggregates are locally visible along the microbial biofilm layers between the laminae. Thin sections taken parallel to the sedimentary layers reveal the presence of vesicles contoured with the same biofilm, micrite, and pyrite framboids (Fig. 4D) similarly to that reported by Belenkaya and Stadnitskaya (1998) and Belenkaya (2003). Ostracod shells, well preserved or fragmented, were also identified in the cement and usually with a partial coating of biofilm. SEM images confirmed the presence of biofilm-coated degassing vesicles

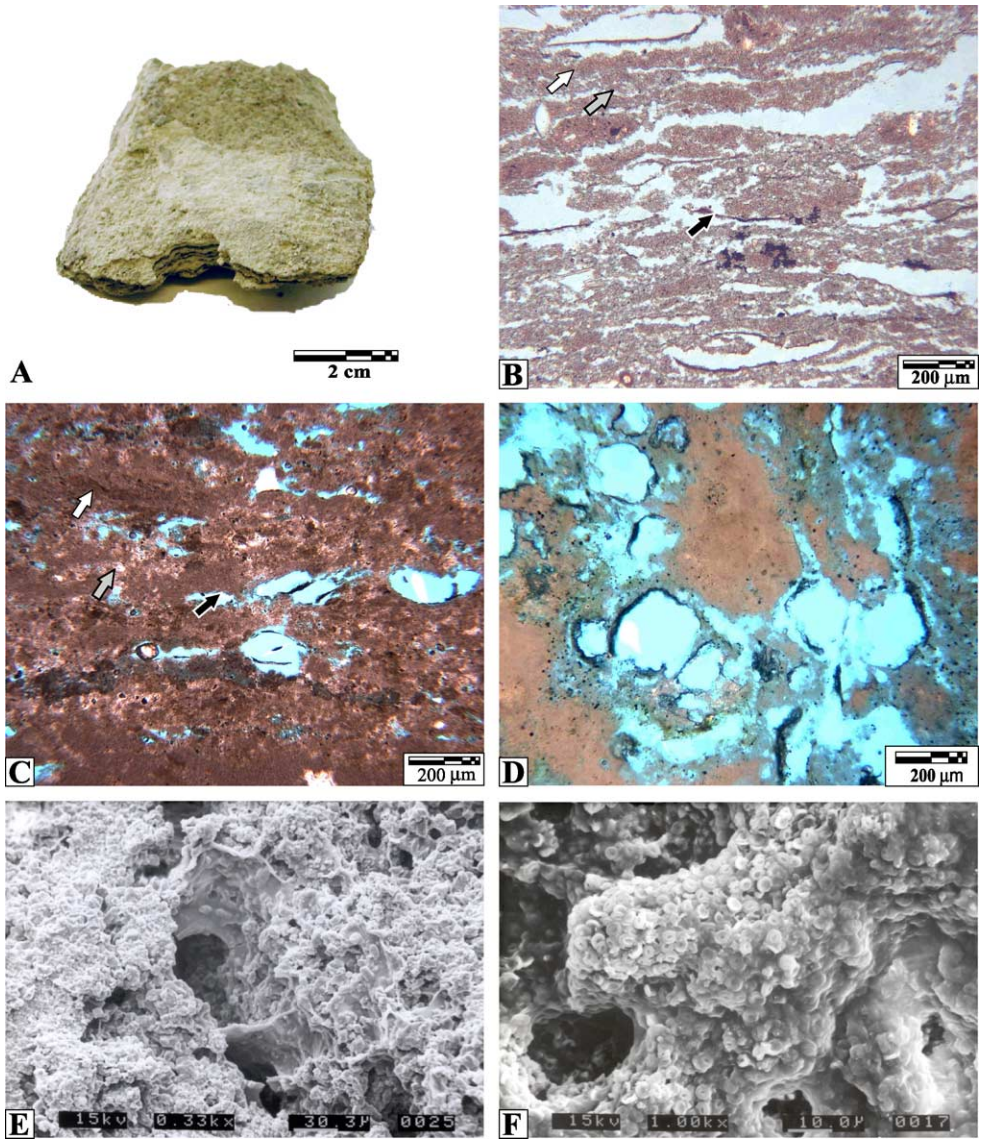

Fig. 4. Authigenic carbonate type U1. (A) Carbonate-cemented fine laminated sedimentary Unit 1; (B) thin section image perpendicular to lamination shows alternating micrite- and clay-rich layers with biofilm and ostracods; (C) thin section image perpendicular to lamination shows irregular alternating micrite- and clay-rich layers with biofilm; (D) thin section image parallel to lamination shows sections of degassing vesicles coated with biofilm (dark colour) and pyrite framboids (dark spots); (E) SEM image with vesicle coated with biofilm; (F) SEM image showing interface laminae with biofilm and coccolith coating. White arrows indicate clay-rich intervals, dark grey arrows indicate the micrite-rich intervals and black arrows point to the biofilm coating.

(Fig. 4E) and coccolith-rich layers mixed with micritic carbonate cement (Fig. 4F). Tubular degassing features oriented perpendicularly to sedimentary lamination were observed and appeared micrite and microbial biofilm coated. In both subtypes U1a and U1b, the slabs can peel off along the clay-rich layers, indicating that they are weak surfaces in contrast to the micrite-rich layers that cement the rock together.

- Type U2—These dark-coloured slabs comprise two subtypes: subtype U2a and subtype U2b (Fig. 5A). Subtype U2a was found in the central part of

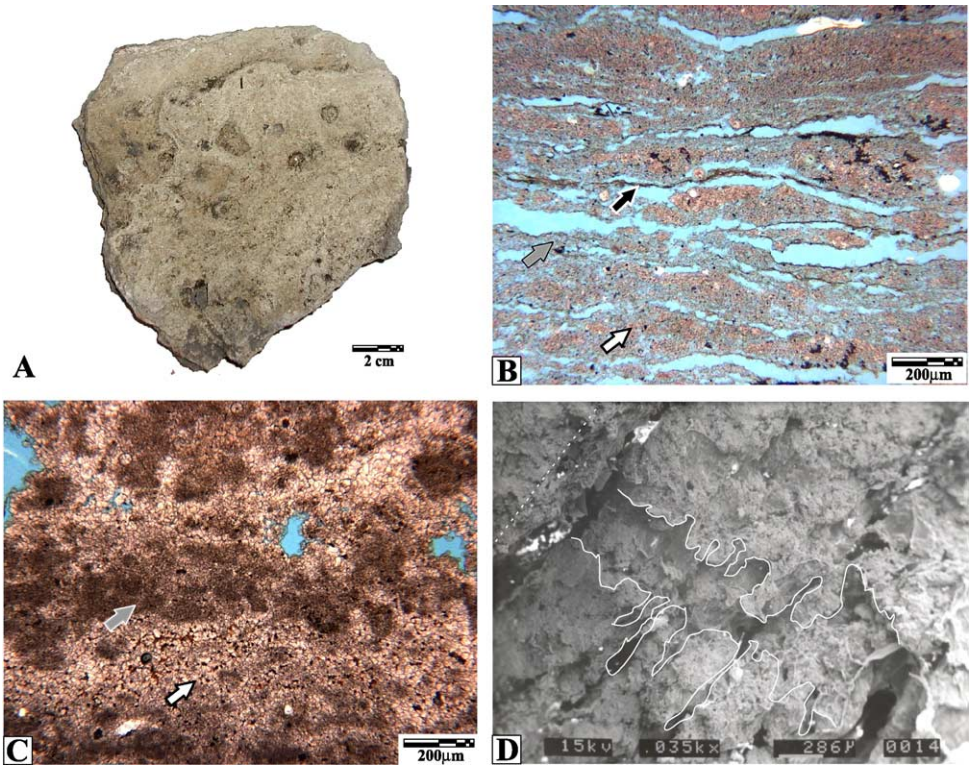

Fig. 5. Authigenic carbonate type U2. (A) Lower surface of a slab subtype U2b, which consists of carbonate-cemented sapropelic Unit 2; note the centimetric degassing vesicles commonly filled with dark microbial mat; (B) thin section image perpendicular to lamination showing clayey layers separated by thin and almost uninterrupted microbial biofilm and micrite-rich layers; (C) thin section image taken perpendicular to lamination of well-cemented slab shows alternated pellets-clay-rich and well-grown calcite crystals; (D) SEM image showing vesicle perpendicularly cross-cutting the sedimentary layers (white solid line) with internal biofilm coating; white dashed line indicates the trend of lamination. White arrows indicate clay-rich intervals; dark grey arrows indicate the micrite-rich intervals and black arrows point to the biofilm coating.

Unit 2 and subtype U2b was retrieved from the upper part and mostly from the bottom part of the same unit. Both the subtypes consist of micrite cemented sapropelic Unit 2 and show a dark colour due to the high organic content present in the sapropel. The flat subtype U2a slabs easily peel off along clay-rich layers, as also observed for subtype U1a. In the case of subtype U2b instead the typical sapropelic layered structure was less visible at the macroscopic scale due to the strong lithification. Small vesicles (from millimetric to 0.5 cm in size) were distinguished on the external surfaces of most of the samples, while the darker slabs, retrieved from the bottom part of Unit 2 (subtype U2b), showed bigger (up 1 cm in size) vesicles. Inside the vesicles, evidence of microbial mat was observed (darker colour or pinkish and brownish). In several instances, thick layers of microbial mats were found on the lower surface of the slabs. The better-cemented slabs were retrieved below thick clayey layers that interrupt the sapropel units, strongly suggesting that the rising of the gas is impeded by these layers. Similar to type U1, thin section observations showed sub-parallel clayey layers separated by thin and almost continuous microbial biofilm and micrite-coccolith-rich layers (Fig. 5B). Exceptionally well cemented slabs, with a virtually pore-free fabric, show well grown calcite crystals between the pellet-clay-rich layers (Fig. 5C). Framboidal pyrite crystals are commonly concentrated along the micrite-biofilm-rich layers and within the degass-

ing vesicles that cross-cut the clay-rich layers. Ostracods were observed in greater amounts than in type U1 and were mostly horizontally oriented along the sedimentary layers. Degassing-like features, perpendicularly cross-cutting the sedimentary layers, are commonly observed with an internal biofilm coating (Fig. 5D).

- Type U3—This type consists of only one single sample composed of poorly micrite-cemented finely laminated Unit 3. Under the microscope, well-defined alternating darker and lighter laminae were observed, the surfaces of which were traced by pyrite framboids. SEM microscopy highlights the presence of microbial biofilm. Despite the poor cementation, the porosity of the sample is very low.
- Type MB–Carbonate cemented mud breccia (type MB) was retrieved at several stations from the Kazakov mud volcano (Fig. 6A). The underwater TV survey and the samples collected show mud breccia crust pavements either on the floor, or capped and cemented together with semi-lithified sedimentary Unit 1 (cemented subtype U1a), or by thicker micritic slabs (type MSa, see following description). These brownish grey fragments of type MB were mostly friable and irregularly shaped. Carbonate cement is coarser if compared with that observed in the previous slabs, and binds the fine fraction of the matrix and the mud breccia clasts of different size (millimetric to centimetric), roundness, and lithology together. Larger calcite crystals commonly appear around the numerous pores and the degassing features present in the mud breccia deposits (Fig. 6B). Pyrite framboids were mostly observed around the degassing vesicles and in the vicinity of the microbial biofilm (Fig. 6C).
- Type MS—Type MS comprises two subtypes: subtype MSa and subtype MSb. Both the subtypes look petrographically similar, consisting of struc-

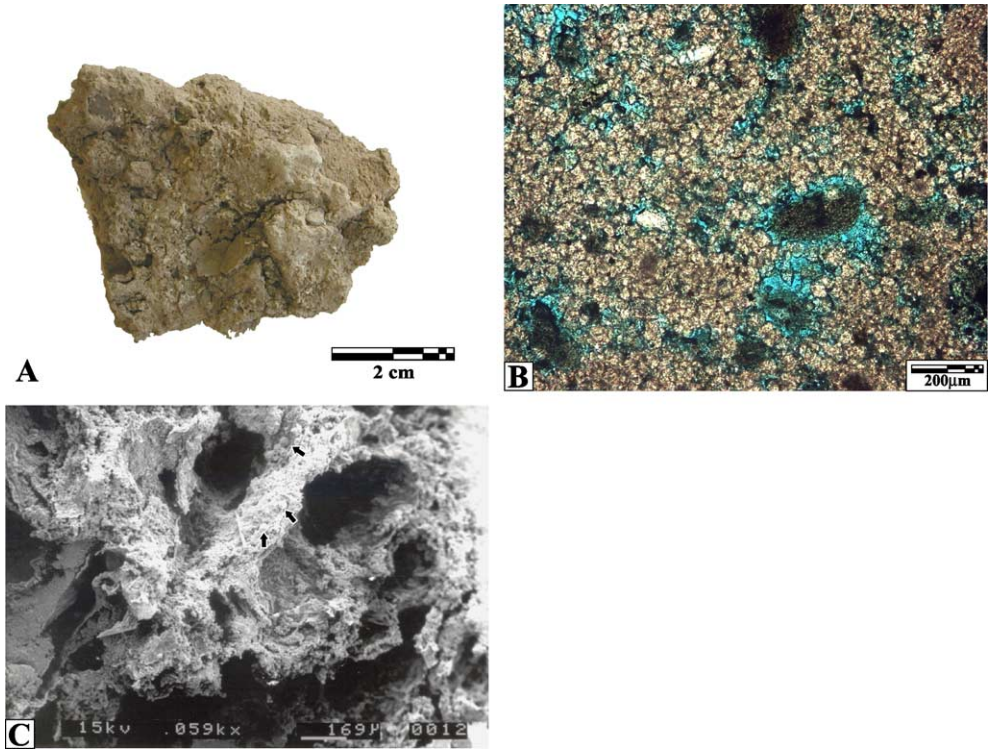

Fig. 6. Authigenic carbonate type MB. (A) Irregularly shaped fragment of carbonate-cemented mud breccia showing fine matrix and clasts; (B) thin section image showing detail of well grown calcite crystals that precipitated around a larger degassing features; (C) SEM image showing degassing vesicles coated with biofilm and pyrite framboids (black arrows indicate some of the framboids around one of the vesicles).

tureless micrite-cemented clayey and pelletoidal fraction with rare microfossils. During the underwater TV survey, Subtype MSa (Fig. 7A) was observed on the sea floor as grey smooth slabs clearly rising above the surrounding sediment, sometimes for several centimetres and often capping mud breccia sediment (Fig. 7B). The top external surfaces appear very porous and covered by microvesicles, which coating suggests microbial activity possibly linked to seepage. In the areas where cavities and the microvesicles are predominant, thin section observations reveal large amounts of pyrite framboids, small sparite crystals, and biofilm coating (Fig. 7C). SEM microscopy

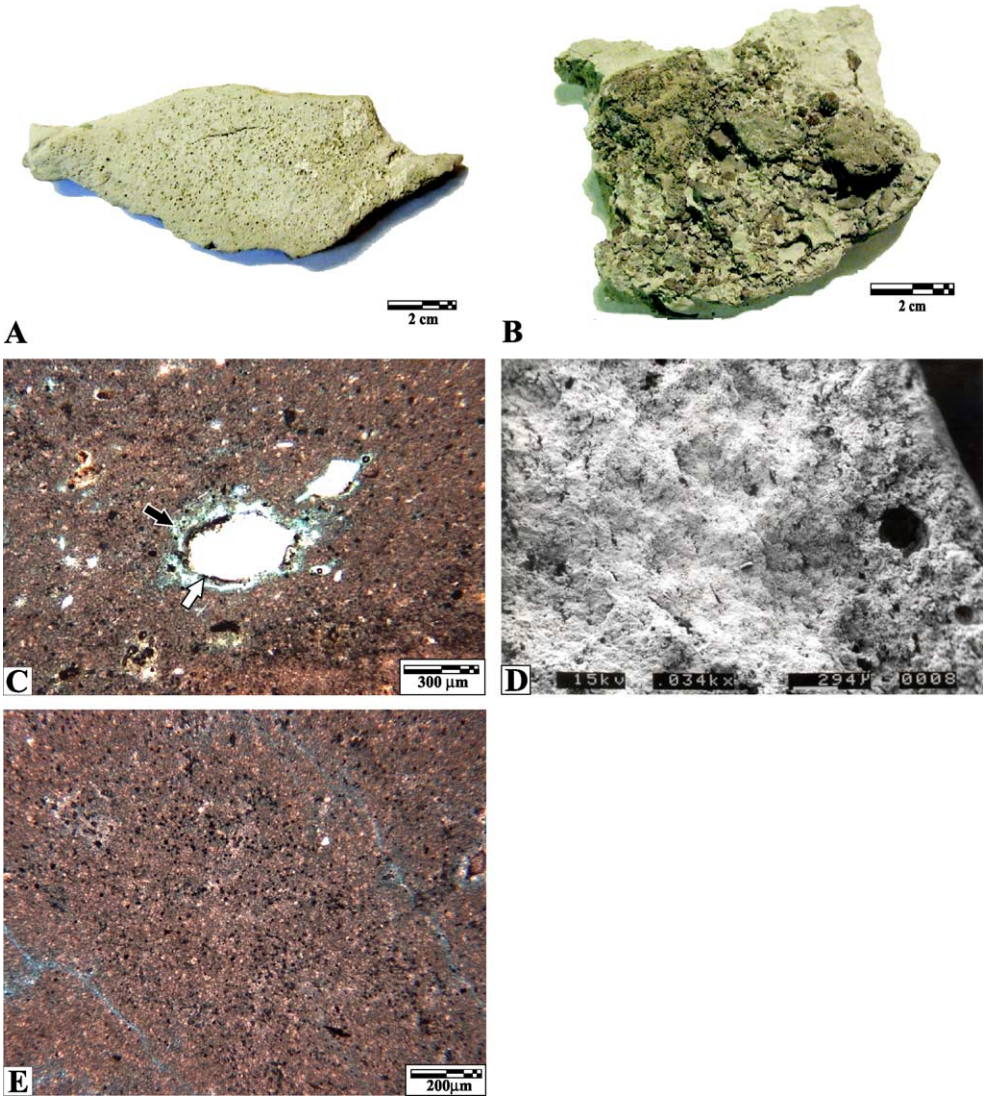

Fig. 7. Authigenic carbonate type MS. (A) Upper surface of smoothed slab subtype MSa; visible microvesicles often filled with microbial mat; (B) lower surface of a slab showing cemented mud breccia sediment (type MB); the upper surface shows authigenic carbonate Subtype MSa; (C) thin section image showing a microvesicle with high concentration of pyrite framboids (dark clots), micrite (black arrow), and biofilm (white arrow); (D) SEM image showing micritic texture with examples of microvesicles on the right side of the image; (E) thin section image showing the micritic texture and the pervasive pyrite framboids.

clearly shows the presence of cavities and vesicles in the internal structure, conferring a light weight to the sample (Fig. 7D). Subtype MSb consisted of tabular-shaped samples retrieved below thin homogeneous layers of pure clay cross cutting Unit 3. The biggest samples were found in slumped bodies within Unit 3; they appeared with irregular and smoothed shape similar to that described for subtype MSa and revealed thin microbial remains coating the external surface. No microvesicles, either on the external surfaces or in the internal structure, were observed, suggesting compaction and gradual infill of the pores by the micritic cement. Pervasive pyrite framboids were observed throughout the samples (Fig. 7E).

5.4.2. Mineralogy of the carbonates

Compositional analyses of the carbonates revealed three different mineralogical types of cement: high Mg calcite (HMC, with $MgCO_3$>5 mol%), low Mg calcite (LMC, with MgCO3 from 0 to 4 mol%), and dolomite (DOL) in one instance. The siliciclastic admixture in the samples has been removed in the calculations and all the results normalised to 100% (Table 1). The percentage distribution of the cements indicates that the majority of the carbonate cements consist of HMC (authigenic carbonate), while variations in LMC% are ascribed to the presence of biogenic carbonate (e.g., coccoliths in type U1) as confirmed by SEM microprobe analyses.

5.4.3. Oxygen and carbon stable isotopes on authigenic carbonates

Samples retrieved from the same structure share common or comparable stable isotope values regardless of the slab type (Table 1). Most of the samples analysed can be divided into two main clusters (Fig. 8).

The first group includes the samples from Area 1 (stations BS-306 and BS-308), from the diapiric structure sampled at station BS-324, and from the NIOZ and Odessa mud volcanoes (Area 3). These are characterised by $\delta^{13}C$ on average lower than −40‰ and $\delta^{18}O$ values mostly comprised between 2.3‰ and −0.6‰. More detailed observations of Area 1 samples show a downcore increase in ^{13}C depletion for type U1 slabs that shift from a mean $\delta^{13}C$=−43.7‰ to a mean $\delta^{13}C$=−46.5‰. An exception was a single sample of type MS authigenic carbonate that gave a negative $\delta^{18}O$ value (−2.5‰) and isotopically heavier carbon values (from −26.8‰ to −25.6‰) based on replicates.

The second group includes samples from the Vassoevich, Kovalevsky (Area 2) and Kazakov (Area 3) mud volcanoes that showed $\delta^{13}C$ values mostly between −24.5‰ and −15.5‰ and the majority of

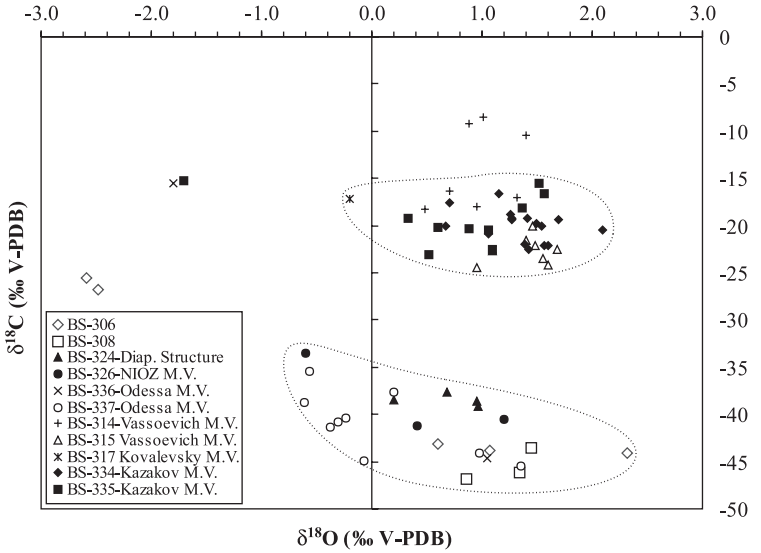

Fig. 8. Carbon and oxygen stable isotope values of authigenic carbonate cements.

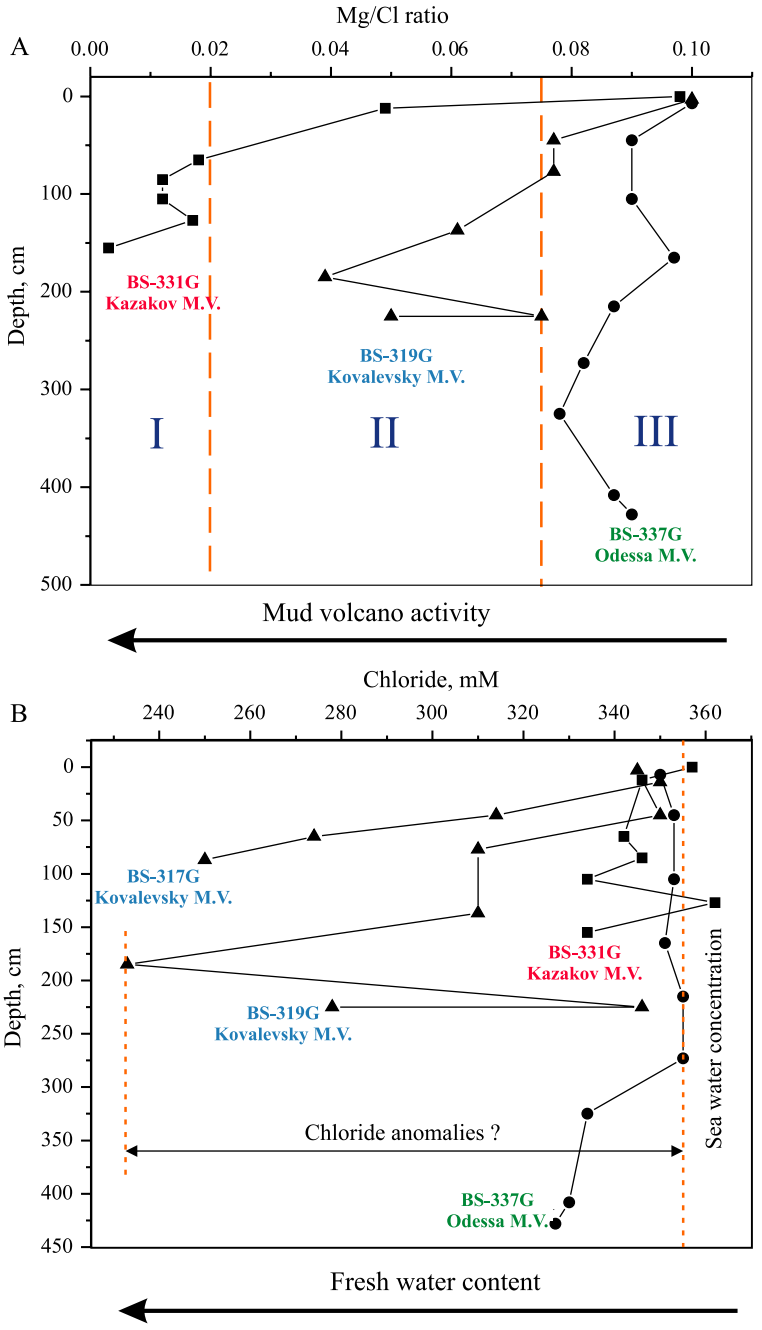

Fig. 9. (A) Distribution of the Mg/Cl ratio in pore waters along cores (station number and structure name are indicated). Three examples of Mg/Cl distribution: I—drastic decrease indicating high content of mud volcano fluids; II—mixed sea water and mud volcano fluids; III—small variation from initial seawater composition; (B) distribution of the chloride (Cl^-) content along cores sampled from mud volcanic structures. The Kovalevsky mud volcano shows big anomalies while the Kazakov and Odessa mud volcanoes show small variation in Cl content. Dotted line indicates seawater concentration (right) and highest anomaly (left).

$\delta^{18}O$ values clustered between −0.2‰ and 2.1‰. In particular, the different types of authigenic carbonate samples from the Vassoevich mud volcano show a downcore increase in ^{13}C depletion and clustered $\delta^{18}O$ values. In fact, type U1 crusts recovered showed moderately depleted $\delta^{13}C$ values (from −8.5‰ to −10.5‰) when compared with subtype U2a retrieved at greater depth (from −16.4‰ to −24.5‰).

5.5. The mud volcanic fluid composition

Attention was focused on the pore water analyses of the Kovalevsky (Area 2), Kazakov, and Odessa mud volcanoes (Area 3).

Fig. 9A shows three examples of differing Mg/Cl distribution. The pore water analyses (I) from the Kazakov mud volcano show a decreasing Mg/Cl ratio with depth while the curve (II) from the Kovalevsky mud volcano reveals a less dramatic decrease. The last curve (III) from the Odessa mud volcano shows small deviations from the initial Mg/Cl seawater ratio.

Water chloride analyses revealed variations in each structure (Fig. 9B). The chloride content for pelagic sediment pore water (sample usually taken at 0-cm depth) and from seawater was similar (approximately 355 mM). The greatest variations were observed in gas hydrate-bearing sediments from the Kovalevsky mud volcano where the values range from 355 to 240 mM. Gas hydrate-bearing intervals of the bottom sediment recovered from the Kazakov and Odessa mud volcanoes were characterised by very small negative chloride anomalies.

6. Discussion

6.1. Carbon sources and the origin of hydrocarbons associated with authigenic carbonates

The two main clusters observed with the stable isotope analyses suggest that the carbonate $\delta^{13}C$ signature is likely to be the result of the mixture in variable proportions of different sources with distinct carbon isotopic composition. These sources comprise carbon primarily derived from methane via AOM (typically ranging between $-90‰ < \delta^{13}C < -30‰$) (Claypool and Kaplan, 1974), from the oxidation of marine organic matter (usually $\delta^{13}C \cong -20‰$) and from inorganic carbon present in the sea water ($0.5‰ < \delta^{13}C < 2‰$) (e.g., Irwin et al., 1977).

The intimate association between methane and carbonate deposits is shown by $\delta^{13}C_{CH_4}$ and $\delta^{13}C_{CaCO_3}$ carbon stable isotope results that reveal a parallel trend for all the studied structures (Fig. 10), confirming previously reported observation by Ivanov et al. (2003). The remarkably constant shift in ^{13}C depletion (around 25–30‰ according to discussed data and around 30–40‰ according to estimations of Ivanov et al., 2003) between carbonates and methane is attributed to a combination of two main factors: transportation processes and kinetic fractionation of carbon during AOM. Although the variability of transport and reaction processes (i.e., advection rates and fractionation factors) at the studied sites is not known, these results suggest that the carbonate crusts were built under fairly constant hydrological and biogeochemical conditions, as suggested by recent biogeochemical modelling (Luff et al., 2004). The two clusters indicated by the $\delta^{13}C_{CH_4}$ suggest at least two possible options. The relatively heavy carbon present in the second cluster of data could be the result of a stronger input of thermogenic gas from depth, suggesting that these structures are more active, or that the roots of the structures are much deeper as suggested by Ivanov et al. (2003). As an alternative, Rayleigh fractionation of carbon at sites where methane is consumed in significant amounts (i.e., via AOM) would result in an enrichment of isotopically heavy carbon in the residual methane (Whiticar and Faber, 1986; Suess and Whiticar, 1989; Whiticar, 1996). Nevertheless, significant microbial activity of SRB and archaea (Stadnitskaia et al., 2003) and hence higher methane consumption, was observed at locations where isotopically lighter methane occurs (i.e., NIOZ and Odessa mud volcanoes). Thus, it seems that AOM does not impact the carbon stable isotope composition of the methane significantly. We conclude that the isotopically heavier methane sampled, e.g., at the Kazakov mud volcano is likely to imply a thermogenic source, rather than isotopic fractionation in a partially or totally closed system.

When considering the features in and above the sapropelic units, a contribution of gas from decayed organic matter present in the sapropel sediment (e.g., Coleman and Ballard, 2001), mixed with deeper-

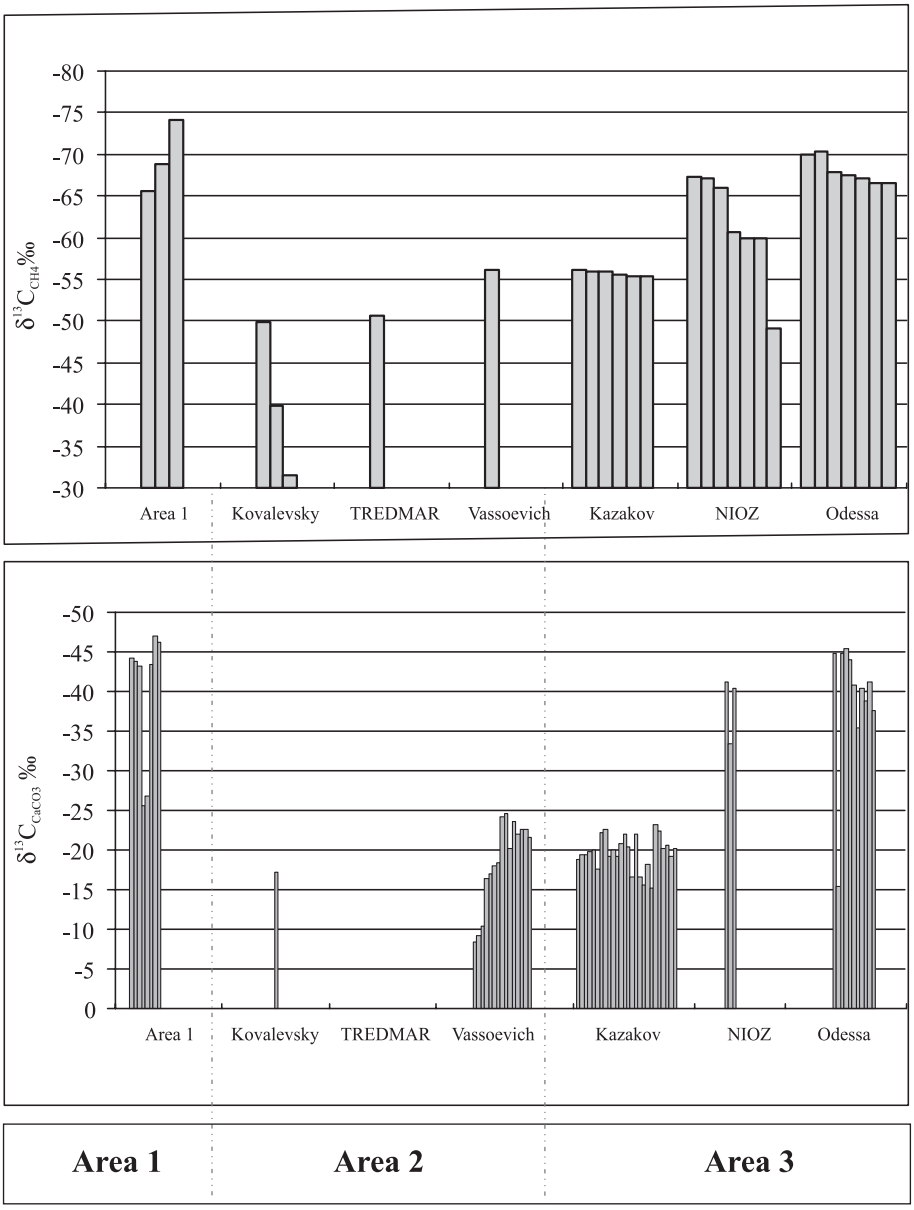

Fig. 10. Comparison of carbon isotopic values from methane (top) and authigenic carbonates (bottom) measured from various structures indicate a similar trend for all the structures. A stronger depletion in ^{13}C is visible for the diapiric structure in Area 1, NIOZ, and Odessa mud volcanoes, while higher values are recorded for the other structures.

rooted gas rising from greater depth, is plausible. However, there is little doubt that the majority of the fluids are rising along the feeder channel of the mud volcanoes. Previous studies (Ivanov et al., 1996) and seismic profiles acquired during this survey (Kenyon et al., 2002) showed that most of the structures have roots located at great depth, below single-channel seismic penetration, suggesting that most probably the deep (4–6 km) roots of the mud volcanoes lie in the Maikopian Formation (and below?). These sediments are highly enriched with organic matter and therefore with a high potential to generate hydro-

carbons (Ivanov et al., 1996). However, hydrocarbon gas compositional analyses indicate that inputs of different hydrocarbons are mixed in the sediments (Fig. 11).

In Area 1, the hydrocarbon gas composition and concentrations analysed from station BS-311G indicate a strong input of hydrocarbons of thermogenic origin in the lower part of the core and a high input of biogenic gas in the upper part where the sapropel unit was described. Similarly, at station BS-308K, gas isotopic analyses reveal strong ^{13}C depletion in the upper part of the core where the sapropel unit was found.

The ratio of methane to heavier hydrocarbons in the mud volcanoes from Area 2 and the methane isotopic values suggests that the studied gas is a mix of gases of biogenic and thermogenic origin. High concentrations of hydrocarbons and the presence of heavy homologues suggest current activity in the volcanoes as also suggested by Ivanov et al. (1996).

The gas compositional analyses of the three mud volcanoes sampled in Area 3 suggest different levels of activity in the structures. The high concentration of the heavy homologues present in the Kazakov mud volcano indicates high maturity for the gas mixture and the combined isotopic values and small amount of nonsaturated hydrocarbons suggest a higher input of thermogenic origin for the migrated hydrocarbon gases. The absence of a hemipelagic veneer covering the mud breccia supports the idea of recent activity of the mud volcano. Similar results were obtained on

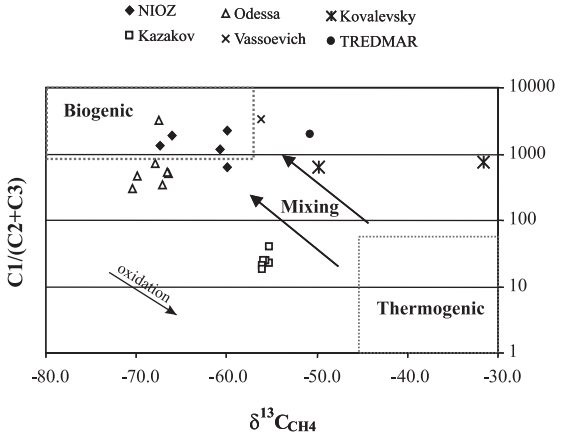

Fig. 11. Combined $\delta^{13}C_{CH_4}$ and hydrocarbon compositional analyses (C1/(C2+C3)) plot for the main structures. Oxidation trend is also indicated.

previous studies from the Kazakov mud volcano sediments (Ivanov et al., 1998; Stadnitskaia and Belenkaya, 1998). The authors described high gas concentration with methane as the dominant component comprising 97.7–99.9% from the total hydrocarbon gases and methane homologues in range of C_2–C_5 and in some cases up to C_6. Analyses from the Odessa mud volcano suggest a higher admixture of microbially mediated methane to the deep-generated heavier gaseous hydrocarbons. The *n*-/*iso*-alkanes ratio indirectly might indicate a dispersal migration mechanism (Bazhenova, 1989) and a low activity of the mud volcano in this particular site. In the case of the NIOZ mud volcano, the absence of alkanes higher than propane (C_3) might indicate different source of the hydrocarbon gases and the lower activity of the mud volcano if compared with the others studied. The isotopic composition of methane indicates its microbial origin.

Other carbon sources (e.g., sea water) are reflected in the stable carbon isotopic signatures of carbonates. For example, in most of the cores described, stratigraphic differences were observed in the authigenic deposits that show a gradual decrease in $\delta^{13}C$ with an increase in depth, suggesting that the shallower slabs contain a relatively higher amount of sea water-derived carbon compared to deeper sited slabs where CH_4 derived carbon dominates. This is particularly evident for the type MS that reveals relatively higher values compared to the other samples from the same location, suggesting the model in which type MS forms very close to the seafloor surface or even directly on the sea floor.

6.2. Authigenic carbonate formation models

Samples that show layered structures (types U1–U3) vary in lithification and degree of porosity but they all share common characteristics. The better-cemented slabs displaying layers of microbial mats on the lower surfaces were commonly found below a few centimetres thick homogeneous clay layers. Recent analyses performed on the microbial mats (mostly form structures sampled in area 3) indicate the presence of archaea and sulphate-reducing bacteria (Stadnitskaia et al., 2003). These observations strongly suggest that the more impermeable layers inhibited the rising gas, thriving microbial activity and

favouring greater carbonate precipitation. Thin section petrography showed a similar pattern, but at smaller scale, with almost continuous microbial biofilm framing thicker clayey laminae. Evidence collected after macro- and microscopic analyses leads to the formulation of a model for authigenic carbonate formation for the layered slabs. Fig. 12A is a schematic summary of the alternations of clay and coccolith-rich layers. The gas (Fig. 12B) will be mostly inhibited by the impermeable clay-rich layers and therefore will preferentially move horizontally, primarily through the more porous, e.g., coccolith-rich layers. The presence of vertical vesicles that cross-cut the clayey layers indicates that the gas can locally seep vertically along microfractures and pore spaces (e.g., Fig. 5D). These vesicles act as pathways for the gas that will saturate and distribute in the coccolith-rich layers. As suggested by other authors for different locations (Boetius et al., 2000; Michaelis et al., 2002; Stadnitskaia et al., 2003), microbial colonies (possibly bacteria and archaea) would then start growing in the gas-saturated layers along the interfaces and the vertical vesicles, inducing the precipitation of authigenic carbonate via methane oxidation and sulphate reduction or from the oxidation of organic matter present in the sediment (Fig. 12C). The pyrite might represent an early diagenetic product linked with the activity of sulphate-reducing bacteria in the anoxic sulphidic zone (Berner, 1984; Hovland et al., 1987; Ritger et al., 1987; Beauchamp and Savard, 1992). Also, the fact that flat laminae of gas hydrates were recovered at the interface between the clayey layers confirms that the gas (either saturated in pore fluids or as free gas) preferentially moves horizontally along these horizons.

Type U2 ^{13}C-depleted slabs showed well-developed and uniform carbonate cementation of the clayey layers. This suggests that a greater amount of carbonate was present at these sites with carbon derived not only from deep-rooted methane and

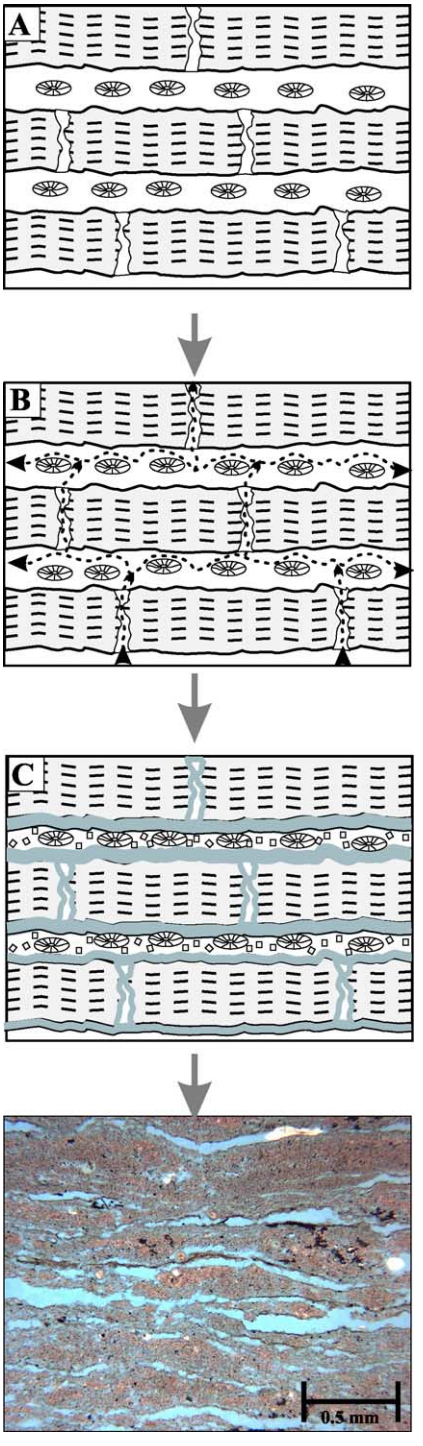

Fig. 12. Suggested model for crust formation. A—planar lamination with alternating coccolith ooze and clayey laminae; B—gas seepage (dotted line) diffusion along more porous coccolith ooze or weak layers; C—formation of biofilm (grey solid line) and calcite (light grey squares) along the interface between the layers and thin section image showing microbial biofilm, pyrite, and sparitic calcite on the interface between the layers.

organic matter but possibly also from in situ microbial methane formation.

The mud breccia pavements described in this study (Kazakov mud volcano) contain cement with calcite crystals better developed than those observed in the other samples. A possible explanation for this could be the larger amount of fluids rising from the feeder channel distributed in the mud breccia deposit, but more likely the higher porosity available in this type of sediment is responsible for the size of the crystals that could grow during time. Similar observations were made by Aloisi et al. (2000) that described voids of carbonate-cemented mud breccia from the Kazan mud volcano displaying large and rhombohedral sparite crystals. Even in this case, these pavements form through the oxidation of methane-charged mud breccia reaching the sea floor. Moreover, numerous samples of mud breccia (type MB) were recovered with type U1 and MSa cemented slabs on top (e.g., Fig. 7B). One unique sample showed the full stratigraphic sequence of the three types cemented together (from the top: type MSa-U1-MB). We suggest that these slabs act as barriers to gas seepage, favouring the precipitation and growth of authigenic carbonate in the underlying mud breccia unit.

The underwater TV survey showed type MS slabs with smoothed surfaces most likely moulded by strong currents flowing around the seepage sites (Fig. 7A). The samples retrieved show an absence of sedimentary structures, high carbonate content, and have no common features with the other cemented units described. These slabs are likely to form very close to the seafloor surface or even directly on the seafloor similarly to the crust type B described by Aloisi et al. (2000) forming pavements that can cover large areas. Assuming a scenario where mud breccia is situated below a succession of hemipelagic units, a combined sequence of carbonate crusts is shown in Fig. 13.

All the Black Sea authigenic carbonate analysed revealed the presence of calcite (with predominance of HMC). At seepage sites, the precipitation of calcite is promoted over aragonite when low sulphate concentrations occur (Burton, 1993; Naehr et al., 2000; Aloisi et al., 2002; Luff and Wallmann, 2003). Conditions similar to these are encountered in the Black Sea that is not only less saline than the normal

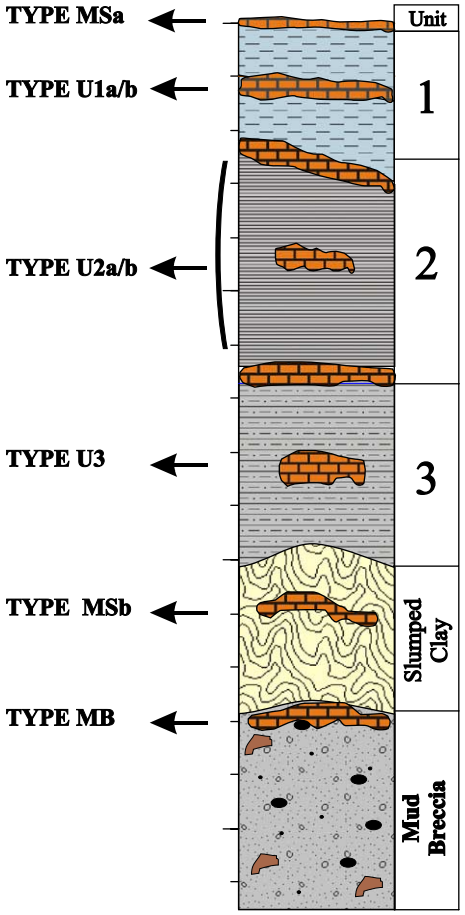

Fig. 13. Sequence of carbonate crusts retrieved (brick pattern) and related lithological units. From the top: subtype MSa, observed with the underwater TV camera and supposed to form on the seafloor; subtype U1a–b, cemented sedimentary Unit 1; subtype U2a–b, cemented sedimentary Unit 2; type U3, cemented sedimentary Unit 3; subtype MSb, retrieved from the slumped clayey intervals within Unit 3; type MB, cemented mud breccia observed either on the seafloor (occasionally with overlying type U1 or subtype MSa), or below the sedimentary units.

oceans but the sulphate concentration averages 18 mM, compared with an average of 28.9 mM for the ocean (Murray et al., 1991). Aragonite, usually observed at many seepage sites, was never detected in the present study.

An attempt to calculate the temperatures of formation of the authigenic carbonates was done applying the fractionation equation of Friedman and O'Neil (1977) and assuming isotopic equilibration with a $\delta^{18}O$ fluid composition of −1.65‰ V-SMOW

(Swart, 1991). The equilibration temperatures were calculated for the two extreme $\delta^{18}O$ values recorded (−0.5‰ and 2.5‰). The four values with $\delta^{18}O$ ranging between −2.5‰ and −1.5‰ were disregarded in this calculation. An average value of the oxygen results was calculated (=0.96‰) as well as the standard deviation (=±0.66‰). The two extreme oxygen values reveal precipitation temperatures between 12 and 0 °C approximately, while the average values is 9 °C, which is the actual sea floor temperature in the Black Sea (e.g., Bohrmann et al., 2003). These results support the model that describes the authigenic carbonates currently precipitating in the near subsurface where interstitial marine pore fluids are present. Nevertheless, we cannot disregard the contribution of mud volcanic fluids that were mixing with the marine pore water during the precipitation of the authigenic carbonates. The dissociation of gas hydrates could explain the presence of cements enriched in ^{18}O that reveal precipitation temperatures close to 0 °C. The negative $\delta^{18}O$ values observed for some of the samples (type MSb) indicate temperatures of carbonate precipitation higher than the actual one or represent the record of less saline waters. This option seems to be the most likely as type MSb was commonly retrieved below Unit 3 and therefore precipitated before the invasion of high salinity waters from the Mediterranean.

6.3. Gas hydrates association with authigenic carbonates

The cores recovered showed that favourable pressure and temperature conditions for the formation of gas hydrates are present at various localities in the near subsurface. It is similarly suggested that in several cases, there is a relationship between the gas that formed the hydrates and the precipitation of authigenic carbonates. In fact, the distribution and the shape of the gas hydrates and the authigenic carbonate appear to be controlled by a combination of segregation processes and by the characteristics of the sedimentary structures. In mud volcanic structures, the subrounded hydrates were found with cemented mud breccia (type MB), with larger calcite crystals in the cavities present in the heterogeneous sediment or in the degassing features. The tabular and leaf-shaped hydrates retrieved in the hemipelagic sediment are remarkably similar to the micritic calcite that precipitates along the sedimentary layer interfaces and that binds the cemented sedimentary units (type U1, U2, U3). It is suggested that, in this case, gas hydrates could locally represent the former phase of methane hydration within the sediment after migration. As documented in several publications, cold seeps can also be fed by the decomposition of gas hydrates that release methane-rich fluids, inducing the precipitation of authigenic carbonates. This phenomenon has been inferred in continental margins (e.g., Bohrmann et al., 1998) and in mud volcanic fields (e.g., Henry et al., 1996; Ivanov et al., 1998). However, in the case of the present study, no strong evidence was recorded to highlight that the dissolution of gas hydrates contributed significantly to the precipitation of authigenic carbonates.

6.4. The fluids involved and their origin

Pore water analyses from the different structures revealed varying fluid compositions. These chemical diversities are attributed to the mixing of three end members: sediment pore water, mud volcano fluids and pure water from gas hydrates. The presence of mud volcano fluids is directly proportional to the mud fluid flow that will mix with the sediment pore water in the uppermost sedimentary layers. Ginsburg et al. (1999), based on pore water studies from the Haakon Mosby mud volcano (Norwegian Sea), showed that the Mg/Cl ratio is an indicator of the mixing of the mud volcano fluid and seawater: the higher this ratio, the smaller will be the fraction of the mud volcano fluid in the water sample. Similar results were also observed in the Ginsburg mud volcano sediments from the Gulf of Cadiz (Mazurenko et al., 2002) and in some structures described herein. In the Black Sea, the principal composition of pore water in the mud volcanoes of the Sorokin Trough has been reported by Belenkaya (2003). The author described the variety of Cl^{-}, Ca^{+}, Mg^{+}, and Al depending on the source of migrating fluids, presence of gas hydrates, and level of activity of mud volcano. The composition of pore water from the Dvurechensky mud volcano was characterised by extremely high chlorinity (three times exceeding of sea water), Ca^{2+} (2 times more than sea water) and a low concentration of

Mg+. This was interpreted to indicate a high level of mud volcanic activity and a deep source of extruded fluids (Ivanov, 1999).

Consistent with the gas analyses, the Mg/Cl ratio suggests that the Kazakov mud volcano has a more active fluid flow compared to the Kovalevsky mud volcano. The comparison of the Mg/Cl ratio and chloride content curves for the Kovalevsky mud volcano suggests an input of fluids with low Mg content. The data for the Odessa mud volcano suggests that it is in a static phase and that fluid flow is not very active at the moment, or it could also indicate that the core was sampled from an inactive area of the mud volcano.

The pore water salinity (more specifically chlorinity) variations have been broadly described as an indirect indicator for the presence of gas hydrates in the sediments (Hesse and Harrison, 1981; Ginsburg et al., 1999). These anomalous chloride concentrations were also observed in the Black Sea mud volcanoes (Ginsburg et al., 1990; Ginsburg and Soloviev, 1998) and explained by the mixing of pore water with fresh water from gas hydrates. Similarly (Fig. 9B), low chloride concentrations were measured in the cores from the Kovalevsky mud volcano (BS-317-G and BS-319-G), in the intervals where gas hydrates were observed. Applying the calculations described by, e.g., Ginsburg et al. (1999) and Mazurenko et al. (2002), a 105 mM anomaly would correspond to approximately 15% gas hydrates in the pore spaces. Nevertheless, such a large amount of hydrates was not observed after retrieval. This could indicate that a substantial volume of gas hydrates decomposed in the sediment due to endothermic reaction or that their size is significantly small. Another factor that has to be considered is that during the upward migration, the deep-sourced mud volcano fluids mixed with fresher near surface waters that characterise the Pleistocene isolation of the Black Sea. This would contribute significantly to reduce the salinity as observed by Manheim and Chan (1974) in several sites all over the Black Sea. Despite the substantial amount of hydrates observed, no significant chloride anomalies were observed in the Odessa and Kazakov mud volcanoes. The absence of anomalies could be explained by the overall high chloride concentrations that characterize the mud volcano fluids (e.g., Dvurechenskii mud volcano) in this region of the Sorokin Trough (Bohrmann and Schenck, 2002; Bohrmann et al., 2003; Drews et al., 2003).

7. Conclusions

Petrographic and geochemical analyses performed on authigenic carbonate, gas samples, and pore waters give results that are consistent with a genetic link between authigenic carbonates and seepage of methane-rich fluids. Five different types of authigenic carbonates are distinguished according to stratigraphic, petrographic, and textural characteristics. The carbon stable isotope composition of authigenic carbonates shows that the primary source of carbon is derived from the AOM mixed with carbon derived from the oxidation of organic matter and from sea water. A proposed formation model for the layered authigenic carbonates (types U1, U2, U3) suggests that AOM was concentrated preferentially at the interface between the clayey layers where authigenic carbonates precipitated. Nonlayered types form close or directly on the seafloor (type MS-MB) or can be capped by overlying slabs or sedimentary units (type MB). Sedimentary structures often control the distribution and the shape of the gas hydrates. Their spatial association with authigenic carbonates, as well as the structural similarities, suggest a genetic connection between the processes of authigenic carbonate and gas hydrate formation. There is a constant shift (~25–30‰) between the $\delta^{13}C$ of methane and authigenic carbonate, suggesting that the investigated carbonates formed under a restricted range of hydrological and geochemical conditions.

Acknowledgments

The authors would like to thank Giovanni Aloisi, Reiner Botz, Gert De Langhe, and Martin Hovland for their critical review of the manuscript and crucial suggestions. Tony Fallick and Andrew Tait (SUERC) are thanked for their support during isotopic analyses; we are grateful to R. Kreulen (NIOZ) for performing methane stable carbon isotopic measurements. We sincerely thank brother Grigorii Akhmanov for his everlasting patience and support during preparation of the manuscript. We would like to

acknowledge the crew and the Scientific Party of the TTR-11 cruise and the UNESCO-MSU Centre for Marine Geosciences.

References

Aloisi, G., Pierre, C., Rouchy, J.M., Foucher, J.P., Woodside, J., 2000. Methane-related authigenic carbonates of eastern Mediterranean Sea mud volcanoes and their possible relation to gas hydrate destabilisation. Earth and Planetary Science Letters 184 (1), 321–338.

Aloisi, G., Bouloubassi, I., Heijs, S.K., Pancost, R.D., Pierre, C., Sinninghe Damste, J.S., Gottschal, J.C., Forney, L.J., Rouchy, J.-M., 2002. CH_4-consuming microorganisms and the formation of carbonate crusts at cold seeps. Earth and Planetary Science Letters 203 (1), 195–203.

Amouroux, D., Roberts, G., Rapsomanikis, S., Andreae, M.O., 2002. Biogenic gas (CH_4, N_2O, DMS) emission to the atmosphere from near-shore and shelf waters of the North-western Black Sea. Estuarine, Coastal and Shelf Science 54 (3), 575–587.

Bazhenova, O.K., 1989. Geochemical Methods of Prospect Work for Marine Oil and Gas Fields. Publishing House of MSU, Moscow (in Russian).

Beauchamp, B., Savard, M., 1992. Cretaceous chemosynthetic carbonate mounds in the Canadian Arctic. Palaios 7 (4), 434–450.

Belenkaya, I., 2003. Influence of hydrocarbon gases on authigenic mineral formation in sediments from cold-seepage areas. Vestnik Moskovskogo Universiteta. Seriâ 4, Geologiâ 36, 15–22 (in Russian).

Belenkaya, I., Stadnitskaya, A., 1998. Authigenic carbonate inclusions in gas saturated sediments of the Black Sea. XXIII General Assembly of the EGS, Abstract book. Nice, France, p. 302.

Berner, R.A., 1984. Sedimentary pyrite formation: an update. Geochimica et Cosmochimica Acta 48 (4), 605–615.

Blinova, V., Ivanov, M.K., Bohrmann, G., 2003. Hydrocarbon gases in deposits from mud volcanoes in the Sorokin Trough. North-Eastern Black Sea 23 (3–4), 250–257.

Boetius, A., Ravenschlag, K., Schubert, C.J., Rickert, D., Widdel, F., Gieseke, A., Amann, R., Jorgensen, B.B., Witte, U., Pfannkuche, O., 2000. A marine microbial consortium apparently mediating anaerobic oxidation of methane. Nature 407, 623–625.

Bohrmann, G., Schenck, S. (Eds.), 2002. Marine Gas Hydrates of the Black Sea (Margasch): R/V Meteor cruise report M52/1. Istanbul (January 2–February 1, 2002). GEOMAR Report, vol. 108, p. 191.

Bohrmann, G., Greinert, J., Suess, E., Torres, M., 1998. Authigenic carbonates from the Cascadia subduction zone and their relation to gas hydrate stability. Geology 7, 647–650.

Bohrmann, G., Abegg, F., Aloisi, G., Artemov, Y., Bialas, J., Broser, A., Drews, M., Fouchet, J.-P., Greinert, J., Heidersdorf, F., Ivanov, M., Blinova, V., Klaucke, I., Krastel, S., Leder, T., Polikarpov, I., Saburova, M., Schellig, F., Schmale, O., Spiess, V., Volkonskaya, A., Weinrebe, W., Zillmer, M., 2002. Mud volcanoes and gas hydrates in the Black Sea—initial results from Meteor Cruise Margash M52/1. 7th meeting on Gas in Marine Sediments and natural marine hydrocarbon seepages, Baku, 7–12, October, pp. 19–20.

Bohrmann, G., Ivanov, M., Foucher, J.P., Spiess, V., Bialas, J., Greinert, J., Weinrebe, W., Abegg, F., Aloisi, G., Artemov, Y., Blinova, V., Drews, M., Heidersdorf, F., Krabbenhoft, F., Klaucke, I., Krastel, S., Leder, T., Polikarpov, G.G., Saburova, M., Schmale, O., Seifert, R., Volkonskaia, A., Zillmer, M., 2003. Mud volcanoes and gas hydrates in the Black Sea: new data from Dvurechenskii and Odessa mud volcanoes. Geo-Marine Letters 23, 239–249.

Bolshakov, A.M., Egorov, A.V., 1987. Methods of phase-semi-balance degassing in gas measuring. Okeanologia 27 (5), 861–862 (in Russian).

Bouriak, S.V., Akhmetjanov, A.M., 1998. Origin of gas hydrate accumulations on the continental slope of the Crimea from geophysical studies. In: Henriet, J.P., Mienert, J. (Eds.), Gas Hydrates: Relevance to World Margin Stability and Climate Change, Geological Society of London Special Publication 137, 215–222.

Burton, E.A., 1993. Controls on marine carbonate cement mineralogy: review and reassessment. Chemical Geology 105 (1/3), 163.

Carson, B., Suess, E., Strasser, J., 1990. Fluid flow and mass flux determination at vent sites on the Cascadia Margin accretionary prism. Journal of Geophysical Research 95, 8891–8897.

Carson, B., Seke, E., Paskevich, V., Holmes, M.L., 1994. Fluid expulsion sites on the cascadia accresionary prism: mapping diagenetic deposits with processed GLORIA imagery. Journal of Geophysical Research 99 (B6), 11956–11969.

Cifci, G., Dondurur, D., Ergun, M., 2002. Sonar and high resolution seismic studies in the Eastern Black Sea. Turkish Journal of Earth Sciences 11 (1), 61–81.

Claypool, G.E., Kaplan, I.R., 1974. The origin and distribution of methane in marine sediments. Natural Gases in Marine Sediments. Plenum, New York, pp. 99–139.

Coleman, D.F., Ballard, R.D., 2001. A highly concentrated region of cold hydrocarbon seeps in the Southeastern Mediterranean Sea. Geo-Marine Letters 21 (3), 162–167.

Coplen, T.B., 1994. Reporting of stable hydrogen, carbon, and oxygen isotopic abundances. Pure and Applied Chemistry 66 (2), 273.

Craig, H., 1957. Isotopic standards for carbon and oxygen and correction factors for mass spectrometric analyses of carbon dioxide. Geochimica et Cosmochimica Acta 12, 133–149.

Degens, E.T., Ross, D.A., 1972. Chronology of the Black Sea over the last 25,000 years. Chemical Geology 10, 1–16.

Drews, M., Schmaljohann, R., Wallmann, K., 2003. Geochemistry and microbiology at gas hydrate and mud volcano sites in the Black Sea. Geophysical Research Abstracts 5, 14735.

Ergun, M., Dondurur, D., Cifci, G., 2002. Acoustic evidence for shallow gas accumulations in the sediments of the Eastern Black Sea. Terra Nova 14 (5), 313–320.

Friedman, I., O'Neil, J.R., 1977. Compilation of stable isotope fractionation factors of geochemical interest. In: Fleisher, M. (Ed.), Data of Geochemistry, 6th edn. USGS Prof. Paper, vol. 44-KK, p. 12.

Gieskes, J.M., Gamo, T., Brumsack, H., 1991. Chemical methods for interstitial water analysis aboard Joides Resolution. ODP, Texas A & M University, Tech. Note, vol. 15, p. 60.

Ginsburg, G.D., Soloviev, V.A., 1998. Submarine Gas Hydrates. VNIIOkeangeologia. Norma Publishers, St. Petersburg, Russia, p. 216.

Ginsburg, G.D., Kremlev, A.N., Grigor'ev, M.N., Larkin, G.V., Pavlenkin, A.D., Saltykova, N.A., 1990. Filtrogenic gas hydrates in the Black Sea (21 voyage of the research vessel "Evpatoriya"). Sov. Geol. Geophys. (Geol Geofiz.) 31 (3), 8–16 (in Russian).

Ginsburg, G.D., Milkov, V.A., Soloviev, V.A., Egorov, A.V., Cherkashev, G.A., Vogt, P.R., Crane, K., Lorenson, T.D., Khutorsky, M.D., 1999. Gas hydrate accumulation at the Haakon Mosby Mud Volcano. Geo-Marine Letters 19 (1/2), 57–67.

Gulin, S.B., Polikarpov, G.G., Egorov, V.N., 2003. The age of microbial carbonate structures grown at methane seeps in the Black Sea with an implication of dating of the seeping methane. Marine Chemistry 84 (1–2), 67–72.

Henry, P., Le Pichon, X., Lallemant, S., Lance, S., Martin, J.B., Foucher, J.-P., Fiala-Médioni, A., Rostek, F., Guilhaumou, N., Pranal, V., Castrec, M., 1996. Fluid flow in and around a mud volcano field seaward of the Barbados accretionary wedge: results from Manon cruise. Journal of Geophysical Research 101 (B9), 20297–20323.

Hesse, R., Harrison, W., 1981. Gas hydrates (clathrates) causing pore-water freshening and oxygen isotope fractionation in deep-water sedimentary section of terrigenous continental margins. Earth and Planetary Science Letters 55, 453–462.

Hovland, M., Talbot, M.R., Qvale, H., Olaussen, S., Aasberg, L., 1987. Methane-related carbonate cements in pockmarks of the North Sea. Journal of Sedimentary Petrology 57 (5), 881–892.

Irwin, H., Curtis, C., Coleman, M., 1977. Isotopic evidence for source of diagenetic carbonates formed during burial of organic-rich sediments. Nature 269, 209–213.

Ivanov, M.K., 1999. Focused hydrocarbon flow on deep-sea continental margins. DSc thesis, Moscow State University, 222 pp. (in Russian).

Ivanov, M.K., Konyukhov, A.U., Kulnitskii, L.M., Musatov, A.A., 1989. Mud volcanoes in deep part of the Black Sea. Vestnik MGU Serie de Geología 3, 21–31 (in Russian).

Ivanov, M.K., Limonov, A.F., Woodside, J. (Eds.), 1992. Initial results of the Training Through Research Cruise of R/V Gelendzhik (June–July 1991). Geological and geophysical investigations in the Mediterranean and the Black Sea, UNESCO Reports in Marine Science 56, 208 pp.

Ivanov, M.K., Limonov, A.F., van Weering, T.C.E., 1996. Comparative characteristics of the Black Sea and Mediterranean Ridge mud volcanoes. Marine Geology 132 (1–4), 253–271.

Ivanov, M.K., Limonov, A.F., Woodside, J.M., 1998. Extensive deep fluid flux through the sea floor on the Crimean continental margin (Black Sea). In: Henriet, J.P., Mienert, J. (Eds.), Gas Hydrates: Relevance to World Margin Stability and Climate Change, Geological Society of London Special Publication 137, 195–214.

Ivanov, M.V., Pimenov, N.V., Rusanov, I.I., Lein, A.Y., 2002. Microbial Processes of the Methane Cycle at the North-western Shelf of the Black Sea. Estuarine, Coastal and Shelf Science 54 (3), 589–599.

Ivanov, M., Stadnitskaia, A., van Weering, T., Kreulen, R., Blinova, V., Kozlova, E., Poludetkina, E., 2003. Composition and possible source of hydrocarbon gases in cold seeps of the deep Black Sea. EGS-AGU-EUG Joint Assembly, Nice, France.

Jeffery, P., Kipping, P., 1976. Analysis of Gases by the Methods of Gas Chromatography, Khimiya, Moscow, pp. 99–101.

Kenyon, N.H., Ivanov, M.K., Akhmetzhanov, A.M., Akhmanov, G.G. (Eds.), 2002. Geological Processes in the Mediterranean and Black Seas and North East Atlantic, Technical Series-Intergovernmental Oceanographic Commission, vol. 62, 123 pp.

Konyukhov, A., Ivanov, M., Kulnitskii, L., 1990. On mud volcanoes and gas hydrates in the deep Black Sea Basin. Litologiâ I Poleznye Iskopaemye 3, 12–23 (in Russian).

Kruglyakova, R.P., Prokoptzev, G.P., Berlizeva, N.N., 1993. Gas-hydrates in the Black Sea as potential hydrocarbon source. Razvedka I Ohrana Nedr 12, 7–10 (in Russian).

Le Pichon, X., Foucher, J.P., Boulegue, J., Henry, P., Lallemant, S., Benedetti, E.L., Avedik, F., Mariotti, A., 1990. Mud volcano field seaward of the Barbados accretionary complex: a submersible survey. Journal of Geophysical Research 95 (B6), 8931–8943.

Lein, A., Pimenov, N., Guillou, C., Martin, J.-M., Lancelot, C., Rusanov, I., Yusupov, S., Miller, Y., Ivanov, M., 2002. Seasonal dynamics of the sulphate reduction rate on the north-western Black Sea shelf. Estuarine, Coastal and Shelf Science 54 (3), 385–401.

Limonov, A.F., Woodside, J., Ivanov, M.K. (Eds.), 1994. Mud Volcanism in the Mediterranean and Black Sea and Shallow Structure of the Eratostene Seamount. Initial Results of the Geological and Geophysical Investigations during the Third "Training Through Research" Cruise of the R/V Gelendzhik (June–July, 1993), UNESCO Reports in Marine Science, vol. 64, 173 pp.

Limonov, A.F., van Weering, T.C.E., Kenyon, N.H., Ivanov, M.K., Meisner, L.B., 1997. Seabed morphology and gas venting in the Black Sea mudvolcano area: observations with the MAK-1 deep-tow sidescan sonar and bottom profiler. Marine Geology 137 (1–2), 121–136.

Luff, R., Wallmann, K., 2003. Fluid flow, methane fluxes, carbonate precipitation and biogeochemical turnover in gas hydrate-bearing sediments at Hydrate Ridge, Cascadia Margin: numerical modelling and mass balances. Geochimica et Cosmochimica Acta 67, 3403–3421.

Luff, R., Wallmann, K., Aloisi, G., 2004. Physical and biogeochemical constraints on carbonate crust formation at cold vent sites: significance for fluid and methane budgets and chemosynthetic biological communities. Earth and Planetary Science Letters 221, 337–353.

MaCrea, J.M., 1950. On isotope chemistry of carbonates and paleotemperature scale. Journal of Chemical Physics 18, 849–857.

Manheim, F.T., Chan, K.M., . Interstitial waters of the Black Sea sediments: new data in review. In: Degens, E.T., Ross, D.A. (Eds.), The Black Sea—Geology, Chemistry and Biology, American Association of Petroleum Geologists Memoir 20, 155–180.

Mazurenko, L.L., Soloviev, V.A., Belenkaya, I., Ivanov, M.K., Pinheiro, L.M., 2002. Mud volcano gas hydrates at the Gulf of Cadiz. Terra Nova 14, 321–329.

Mazurenko, L.L., Soloviev, V.A., Gardner, J.M., Ivanov, M.K., 2003. Gas hydrates in the Ginsburg and Yuma mud volcano sediments (Moroccan Margin): results of chemical and isotopic studies of pore water. Marine Geology 195 (1–4), 201–210.

McDuff, R.E., 1985. The chemistry of interstitial waters, deep sea drilling-chloride titration, $AgNO_3$. Project leg 86. Initial Report of the DSDP 86, 675–687.

Michaelis, W., Seifert, R., Nauhaus, K., Treude, T., Thiel, V., Blumenberg, M., Knittel, K., Gieseke, A., Peterknecht, K., Pape, T., Boetius, A., Amann, R., Jørgensen, B., Widdel, F., Peckmann, J., Pimenov, N.V., Gulin, M.B., 2002. Microbial reefs in the Black Sea fueled by anaerobic oxidation of methane. Science 297, 1013–1015.

Murray, J.W., Top, Z., Özsoy, E., 1991. Hydrographic properties and ventilation of the Black Sea. Deep Sea Research 38 (2), 663–689.

Naehr, T.H., Rodriguez, N.M., Bohrmann, G., Paull, C.K., Botz, R., 2000. Methane-derived authigenic carbonates associated with gas hydrate decomposition and fluid venting above the Blake Ridge Diapir. In: Paull, C.K., Matsumoto, R., Wallace, P.J., Dillon, W.P. (Eds.), Proc. ODP Sci. Resilts, vol. 164. Ocean Drilling Program, College Station, TX, pp. 286–300.

Nikishin, A.M., Korotaev, M.V., Ershov, A.V., Brunet, M.-F., 2003. The Black Sea basin: tectonic history and Neogene–Quaternary rapid subsidence modelling. Sedimentary Geology 156 (1–4), 149–168.

Peckmann, J., Reimer, A., Luth, U., Luth, C., Hansen, B.T., Heinicke, C., Hoefs, J., Reitner, J., 2001. Methane-derived carbonates and authigenic pyrite from the northwestern Black Sea. Marine Geology 177 (1–2), 129–150.

Polikarpov, G.G., Ivanov, M.V., Gulin, S.B., Gulin, M.B., 1993. Deposition of methane carbon in the carbonate chimneys grown in anoxic zone at the Black Sea slope. Proceedings of Ukrainian Academy of Sciences 7, 93–94 (in Russian).

Reznikov, A.A., Muikovskaya, E.P., 1956. Analysis of natural waters and brines. In: Knipovich, Y., Yu, M.V. (Eds.), Analysis of Minerals. State Chemical Publishing, Leningrad, pp. 872–1047. In Russian.

Ritger, S., Carson, B., Suess, E., 1987. Methane-derived authigenic carbonates formed by subduction-induced pore-water expulsion along the Oregon/Washington margin. Geological Society of America Bulletin 98, 147–156.

Ross, D.A., Degens, E.T., 1974. Recent sediments of Black Sea. In: Degens, E.T., Ross, D.A. (Eds.), The Black Sea—Geology, Chemistry and Biology. American Association of Petroleum Geologists, Memoir 20, 183–199.

Ross, D.A., Degens, E.T., Macllvaine, J., 1970. Black Sea: recent sedimentary history. Science 170, 163–165.

Ross, D.A., Neprochnov, Y.P., et al., 1978. Initial Reports of the Deep Sea Drilling Project, vol. 42, Part 2. U.S. Government Printing Office, Washington, 1244 pp.

Ryan, W.B.F., Pitman, W.C., Major, C.O., Shimkus, K., Moskalenko, V., Jones, G.A., Dimitrov, P., Goruer, N., Sakinc, M., Yuece, H., 1997. An abrupt drowning of the Black Sea shelf. Marine Geology 138 (1/2), 119–126.

Sharma, T., Clayton, R.N., 1965. Measurement of $^{18}O/^{16}O$ ratios of total oxygen in carbonates. Geochimica et Cosmochimica Acta 29, 1347–1353.

Shlikov, V.G., Kharitonov, V.D., 2001. On method of quantitative X-ray analysis of mineral composition of the rocks. Geoecology, Engineering, Geology, Hydrogeology. Geocryology 2, 129–140.

Shnukov, E.F., Sobolevskiy, Y.V., Kutniy, V.A., 1995. Unusual carbonate buildups at continental slope of the north-western Black Sea: an apparent consequence of the degassing of sediments. Lithology and Minerals 5, 461–541 (in Russian).

Stadnitskaia, A., Belenkaya, I., 1998. Gas hydrates in the seabed sediments on the Northeastern part of the Black Sea. XIII General Assembly of the EGS, Abstract book. Nice, France, p. 299.

Stadnitskaia, A., Baas, M., Ivanov, M.K., Van Weering, T.C.E., Sinninghe Damste', J.S., 2003. Novel archeal macrocyclic diether core membrane lipids in a methane-derived carbonate crust from a mud volcano in the Sorokin Through, NE Black Sea. Archaea 1, 1–9.

Suess, E., Whiticar, M.J., 1989. Methane-derived CO_2 in pore fluids expelled from the Oregon Subduction Zone. In: O.H. (Ed.), KAIKO Conference Proceedings, 1986, Palaeogeography, Palaeoclimatology, Palaeoecology 71, 119–136.

Swart, P.K., 1991. The oxygen and hydrogen isotopic composition of the Black Sea. Deep Sea Research 38 (Suppl. 2), S761–S772.

Thiel, V., Peckmann, J., Richnow, H.H., Luth, U., Reitner, J., Michaelis, W., 2001. Molecular signals for anaerobic methane oxidation in Black Sea seep carbonates and a microbial mat. Marine Chemistry 73 (2), 97–112.

Tugolesov, D.A., Gorshkov, A.S., Meysner, L.B., Soloviov, V.V., Khakhalev, E.M., Akilova, Y.V., Akentieva, G.P., Gabidulina, T.I., Kolomeytseva, S.A., Kochneva, T.Y., Pereturina, I.G., Plashihina, I.N., 1985. Tectonics of the Mesozoic sediments of the Black Sea basin. 215 pp (in Russian).

Vogt, P.R., Cherkashev, G.A., Ginsburg, G.D., Ivanov, G., Milkov, A., Crane, K., Lein, A., Sundvor, E., Pimenov, N., Egorov, A., 1997. Haakon Mosby Mud Volcano provides unusual example of venting. EOS 78 (549), 556–557.

Whiticar, M.J., 1996. Isotope tracking of microbial methane formation and oxidation. In: Adams, D.D., Crill, P.M., Seitzinger, S.P. (Eds.), Cycling of Reduced Gases in the Hydrosphere, Mitteilung (communications), Internationalen Vereinigung für Theoretische und Angewandte Limnlogie. Schweizerbart'sche Stuttgart, Germany, vol. 23, pp. 39–54.

Whiticar, M.J., Faber, E., 1986. Methane oxidation in sediments and water column environments—isotope evidence. Organic Geochemistry 10, 759–768.

Woodside, J., Ivanov, M.K., Limonov, A.F. (Eds.), 1997. Neotectonics and Fluid Flow Through Seafloor Sediments in the Eastern Mediterranean and Black Sea. Preliminary results of Geological and Geophysical Investigations During the ANAXIPROBE/TTR-6 Cruise of R/V Gelendzhik July–August, 1996. Technical Series-Intergovernmental Oceanographic Commission, vol. 48. 226 pp.